Applied Mathematical Modelling 122 (2023) 456–476

Contents lists available at ScienceDirect

Applied Mathematical Modelling

journal homepage: www.elsevier.com/locate/apm

A minimal mathematical model to study insulin synthesis and secretion process

Abhijit Paul, Jayendrajyoti Kundu, Samrat Chatterjee*

Complex Analysis Group, Translational Health Science and Technology Institute, NCR Biotech Science Cluster, Faridabad-Gurgaon Expressway, Faridabad-121001, India

ARTICLE INFO

Article history:
Received 9 December 2022
Revised 4 June 2023
Accepted 9 June 2023
Available online 11 June 2023

Keywords:
Insulin
Glucose-stimulated insulin secretion
Insulin synthesis
Type 2 diabetes
Insulinoma
Insulin granule dynamics

ABSTRACT

Insulin, secreted from pancreatic β-cells, plays a vital role in maintaining glucose homeostasis in our body. In various pathophysiological conditions like diabetes, cancer, etc., this glucose-insulin relationship is altered. However, the underlying mechanisms behind the β-cell malfunctioning under these pathophysiological conditions remain a research topic. The current study aimed to explore the key factors responsible for impaired insulin secretion from β-cells. We studied insulin synthesis and secretion processes through a minimal mathematical model incorporating insulin mRNA, proinsulin pool, and insulin granules. Defects in the insulin granule trafficking and exocytosis processes hamper first- and second-phase insulin secretion and might be one of the main reasons for β-cell dysfunction in type 2 diabetes. The long-term effect of abnormal insulin synthesis could hamper insulin secretion and make the scenario more critical, causing complete insulin loss inside the β-cells. Besides, uncontrolled insulin synthesis could increase basal insulin secretion and drive toward fasting hypoglycemia. The present study also hypothesizes that regulation of insulin synthesis through targeting transcription and translation is a potential therapeutic strategy for controlling impaired insulin secretion.

1. Introduction

Insulin is an endocrine peptide hormone essential for maintaining glucose homeostasis in our body and is produced generally from the β-cells of the pancreatic islets. It controls the blood glucose levels by promoting cellular uptake of glucose into the liver, fat, and skeletal muscle and regulating the metabolism of carbohydrates, lipids, and protein [1]. The high blood insulin concentration also strongly inhibits glucose production and secretion by the liver [1]. Glucose is the primary stimulus for insulin release from pancreatic β-cells, though other macronutrients (fatty acids and amino acids), hormones, and neural input may augment this response [2,3]. In various pathophysiological conditions like diabetes, cancer, etc., this glucose-insulin dose-response relationship is dysregulated and ultimately affects the body's homeostasis. At the initial stage of type 2 diabetes (T2D), insulin resistance-induced hyperglycemia impairs β-cell function and eventually results in reduced glucose-stimulated insulin secretion (GSIS) [4]. Although this is a major cause of developing T2D, the intrinsic mechanism underlying the β-cell failure remains largely unclear [5]. Conversely, insulinoma cells, a rare type of neuroendocrine pancreatic tumour cell, secrete insulin autonomously [6]. The insulinoma cells can not suppress insulin secretion under low glucose conditions, leading to fasting hypoglycemia [6,7].

* Corresponding author.
E-mail address: samrat.chatterjee@thsti.res.in (S. Chatterjee).

https://doi.org/10.1016/j.apm.2023.06.012
0307-904X/

Insulin secretion from β-cells is mainly biphasic and requires accelerated cellular uptake of glucose, and its metabolism [8–10]. The first phase, known as the triggering pathway [11], lasts 4–8 min. It involves a series of cellular events, such as uptake of glucose through glucose transporters 2 (GLUT2), cytoplasmic and mitochondrial metabolism of glucose, increases in cytoplasmic ATP/ADP concentration, closure of ATP-sensitive potassium channels (K_{ATP}), cell membrane depolarization, Ca^{2+} influx through voltage-gated Ca^{2+} channels and exocytosis of the 'primed' insulin granules [12,13]. The second phase of insulin secretion, known as the amplifying pathway [11], can be sustained for up to several hours, depending on blood glucose levels. This phase also depends on glucose metabolism and intracellular rise of Ca^{2+} content and also involves signals important for recruiting, priming, and docking insulin granules [10]. Glucose is also a main physiological regulator of insulin production and influences the production by multiple mechanisms, including the proinsulin gene transcription, mRNA stability, and the translational process [10,13]. In the short term ($<$4 h), the insulin production increases due to augmented translation of pre-existing mRNA; however, the prolonged stimulus ($>$12 h) also increases the mRNA expression of the proinsulin gene either through transcription and/ or stabilizing the mRNA [14–16]. Thus, any impairment of these processes can directly influence the insulin level and leads to dysregulation in glucose homeostasis. However, there is still a lack of knowledge on the mechanisms regulating glucose-stimulated insulin synthesis and secretion under physiological and pathophysiological conditions [5].

Recently, we investigated the GSIS process to understand the possible factors affecting insulin secretion in the insulin resistance-induced hyperglycemic state [17]. We observed that insulin secretion could be hampered due to the loss in the glucose-evoked rise in cytosolic Ca^{2+} content. The probable mechanisms include the reduced activity of glucokinase (GK), decreased ATP synthesis from glucose metabolism, increased ATP usage rate, overactivity of the K_{ATP} channels, and increased efflux of Ca^{2+}. Even though we found that a diminished calcium-induced exocytosis rate of insulin-containing granules may contribute to T2D development, the whole mechanisms still need to be fully explored. For instance, the rate of insulin production and dynamics of formation and trafficking to the cell membrane of insulin granules were not studied. There are also models on insulin granule dynamics that studied the defects in amplifying pathways, including translocation from the reserve pool to the immediately releasable pool, suggesting possible other reasons behind the defective insulin secretion [18–21]. However, none has explored the defects in insulin synthesis processes, although these could also cause depletion in insulin granules. It is well-known that chronic hyperglycemia affects the insulin gene expression by reducing promoter activity and levels of two important transcription factors, PDX1 and MAFA, and leads to diminished β-cell insulin content [22].

In the present study, we proposed a simplified model for insulin synthesis and secretion of insulin granules. We incorporated the insulin mRNA as a variable in the model to investigate the consequences of defects in the transcription and translation processes of the insulin gene. One of the aims of the study was to identify parameters that could hamper insulin secretion. Another aim of this study is to capture the important factors responsible for the continuous secretion of insulin by β-cells under low glucose conditions, a condition observed in insulinoma patients. The model was further analyzed to compare insulin synthesis and exocytosis processes in restoring impaired insulin secretion. Finally, the study ends by proposing possible restoration strategies against different β-cells masses.

Glossary

State variables

Symbols	Definition (Equation number where first refer)	Basal values with unit
M	Insulin gene mRNA (Eq. (1))	126,753 tpm
P	The proinsulin pool (Eq. (2))	10
R	The reserve pool (Eq. (3))	10,000
D	The pool of docked granules (Eq. (4))	950
D_{IR}	The pool of immediately releasable granules (Eq. (5))	50
γ	Factor representing ATP-to-ADP ratio (Eq. (6))	γ_b min^{-1}
ρ	Factor representing cytosolic Ca^{2+} concentration (Eq. (8))	ρ_b min^{-1}
Additional variables		
G	Extracellular glucose concentration (Eq. (6))	4.58 mmol/l
ISR	Insulin secretion rate (Eq. (10))	1.6×10^{-3} pmol/(min islet)

2. Formulation of the mathematical model

To capture the insulin synthesis, we here introduced two variables the insulin gene mRNA and the proinsulin pool. Besides, the insulin granules trafficking and exocytosis processes were explored through the dynamics of three intracellular pools of insulin granules: the reserve pool, the pool of docked granules, and the pool of immediately releasable granules. Glucose is the major physiological regulator of the entire system. It regulates insulin gene transcription, mRNA stability, mRNA translation, and the secretion of insulin granules. A schematic diagram of insulin biosynthesis and the formation and secretion of insulin granules processes is presented in Fig. 1 and a minimal model representing schematic diagram is discussed below. The equations are based on the earlier published model [20], which was modified to address the insulin secretion and synthesis process.

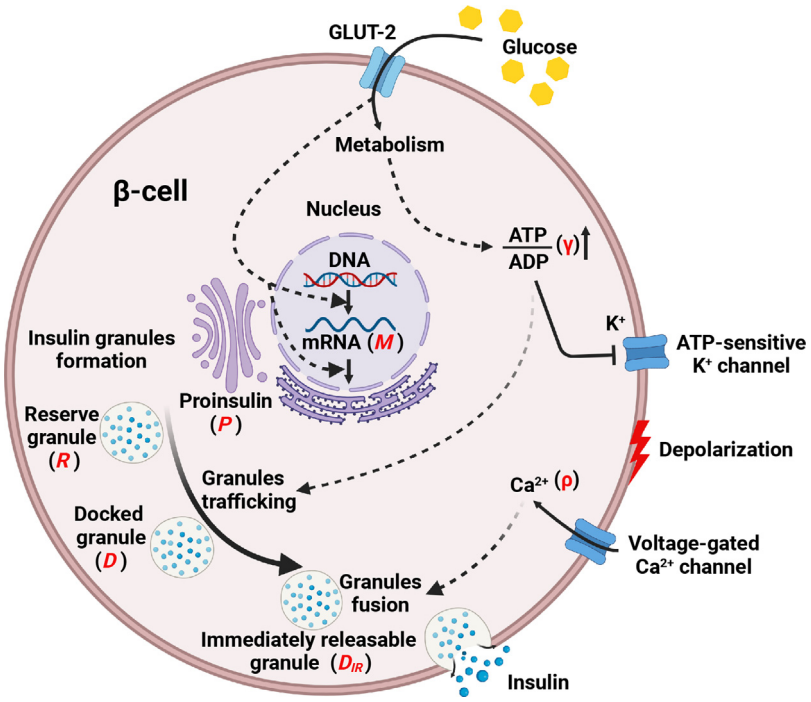

Fig. 1. Schematic diagram of the proposed mathematical model on glucose-stimulated insulin synthesis and secretion process. Here, a pancreatic β-cell is considered where glucose enters the cell via glucose transporters (GLUT-2), which then regulates insulin gene transcription, mRNA stability, mRNA translation, and the secretion of insulin granules through various pathways. The glucose-stimulated insulin synthesis and secretion process was studied here by constructing the dynamical equations for seven key players. These are as follows: 1) insulin gene mRNA, 2) the proinsulin pool, 3) ATP-to-ADP ratio, 4) cytosolic Ca^{2+} concentration, and three intracellular pools of insulin granules: 5) the reserve pool, 6) the pool of docked granules, and 7) the pool of immediately releasable granules. The effect of glucose stimulus was imposed by considering the increased transcription and translation rate and a regulatory function on the dynamics of the ATP-to-ADP ratio.

Let $M(t)$ denote the insulin mRNA level at time t. The transcription rate of the insulin gene is controlled by complex interactions between the transcription factors (PDX1, MAFA, BETA2, and ATF2) and the specific elements within the insulin promoter site [3,26,27]. Glucose enhances the transcription rate through several complementary mechanisms, including the recruitment of transcription factors to regulatory sites, histone modifications, and initiation of transcription [28]. It also increases the stability of insulin mRNA [15]. For simplicity, we considered the transcription rate a constant and a linear term for mRNA degradation. So, the dynamical equation of M is expressed as

$$\frac{dM}{dt} = \alpha_1 - \delta_1 M, \tag{1}$$

where α_1 and δ_1 denote constant transcription rate and a constant degradation rate respectively. It is reported that long-term exposure to glucose stimulus could approximately induce a 2-fold increase in the level of insulin mRNA. So, to capture this phenomenon, we considered the increased values for α_1 and δ_1 for the high glucose model simulation (see Appendix A). The insulin mRNA product encodes preproinsulin (the insulin precursor), which is translated into the rough endoplasmic reticulum (rER) compartment. The synthesis of proinsulin is also a very complex process. It depends on the series of steps, starting from the translational of mRNA, translocation of the products into the rER lumen, the rapid folding, formation of the disulfide bond, and finally, the transportation into the Golgi apparatus [29]. The biosynthesis rate of the pool of proinsulin aggregates ($P(t)$) from the insulin mRNA is expressed as νM, where ν is the rate constant. Similar to the transcription rate, the proinsulin pool formation rate also increases in glucose stimulus. Therefore, a higher value of ν was considered for the high glucose model simulation compared to the low glucose case [14]. The governing equation for P is expressed as

$$\frac{dP}{dt} = \nu M - \delta_2 P - kP\rho D_{IR}, \tag{2}$$

where δ_2 is a degradation rate constant. The last term denotes the formation rate of insulin granules in the trans-Golgi apparatus, a function of pool of proinsulin aggregates ($P(t)$) and the available free granules membrane materials. At the exocytosis of insulin granules, the granule membrane materials become part of the plasma membrane and are successively removed and returned to the trans-Golgi apparatus for recycling. We denoted the rate of granule membrane fusion with the cell membrane by ρD_{IR}, where ρ represents the rate coefficient that accounts for the factors that promote the exocytosis of insulin granules. D_{IR} represents the immediately releasable pool. The dynamical equation for the reserve pool (R) is

expressed as

$$\frac{dR}{dt} = kP\rho D_{IR} - \gamma R, \tag{3}$$

where γR was considered as the conversion rate of reserve pool into the pool of docked granules (D) [20]. The dynamics of the pool of docked granules and pool of immediately releasable pool were taken from Bertuzzi et al. [20], and are expressed as

$$\frac{dD}{dt} = \gamma R - k_1^+(C_T - D_{IR})D + k_1^- D_{IR}, \tag{4}$$

$$\frac{dD_{IR}}{dt} = k_1^+(C_T - D_{IR})D - k_1^- D_{IR} - \rho D_{IR}, \tag{5}$$

where C_T denotes the constant pool of total Ca^{2+} channels. k_1^+ and k_1^-, respectively, are the rate constants of association and dissociation for the binding between docked granule and Ca^{2+} channel. Glucose-stimulated insulin secretion from β-cells is biphasic. The first phase lasts for 4–8 min and involves a series of cellular events; uptake of glucose through glucose transporters 2 (GLUT2); metabolism of glucose; increases in cytoplasmic ATP/ADP concentration; closure of K_{ATP} channels; cell membrane depolarization; Ca^{2+} influx through voltage-gated Ca^{2+} channels and exocytosis of the 'primed' insulin granules [12,13]. The second phase of insulin secretion can be sustained for up to several hours, depending on blood glucose levels. This phase also depends on glucose metabolism and intracellular rise of Ca^{2+} content but also involves signals important for recruiting, priming, and docking the insulin granules [10]. All these are incorporated by taking a simplified dynamics of γ (factor representing ATP-to-ADP ratio), and ρ (factor representing cytosolic Ca^{2+} concentration) [20]. The governing equations of γ is as follows

$$\frac{d\gamma}{dt} = \eta(-\gamma + \gamma_b + \alpha_2(G)), \tag{6}$$

where η is the rate constant and γ_b denotes the basal value of γ at low glucose. The function $\alpha_2(G)$ indicates the response of glucose stimulus [20] and is expressed as

$$\alpha_2(G) = \begin{cases} 0, & G \le G^* \\ \frac{\hat{h}(G-G^*)}{\hat{G}-G^*}, & G^* < G \le \hat{G} \\ \hat{h}, & G > \hat{G} \end{cases} \tag{7}$$

where $\hat{h}$ is the maximal value of α_2 and is achieved at $G = \hat{G}$. The rate equation of ρ depends on γ with increase in the ATP-to-ADP ratio. This leads to the closure of K_{ATP} channels and results in Ca^{2+} influx through voltage-gated Ca^{2+} channels. The dynamical equation for ρ was taken from Bertuzzi et al. [20], and is expressed as

$$\frac{d\rho}{dt} = \zeta\left(-\rho + \rho_b + k_\rho(\gamma - \gamma_b)\right), \tag{8}$$

where ζ is the rate constant and the last term defines the action of γ on ρ. Thus, the simplified model of insulin synthesis and the biogenesis and secretion of insulin granules is proposed by the following system of ordinary differential equation (ODE)

$$\begin{aligned}
\frac{dM}{dt} &= \alpha_1 - \delta_1 M, \\
\frac{dP}{dt} &= vM - \delta_2 P - kP\rho D_{IR}, \\
\frac{dR}{dt} &= kP\rho D_{IR} - \gamma R, \\
\frac{d\gamma}{dt} &= \eta(-\gamma + \gamma_b + \alpha_2), \\
\frac{dD}{dt} &= \gamma R - k_1^+(C_T - D_{IR})D + k_1^- D_{IR}, \\
\frac{dD_{IR}}{dt} &= k_1^+(C_T - D_{IR})D - k_1^- D_{IR} - \rho D_{IR}, \\
\frac{d\rho}{dt} &= \zeta\left(-\rho + \rho_b + k_\rho(\gamma - \gamma_b)\right),
\end{aligned} \tag{9}$$

with the initial conditions $M(0) > 0$, $P(0) > 0$, $R(0) > 0$, $\gamma(0) > 0$, $D(0) > 0$, $D_{IR}(0) > 0$, $\rho(0) > 0$. Insulin secretion rate (ISR) was taken from Bertuzzi et al. [20], and is denoted by

$$[ISR](t) = I_0 \rho D_{IR}(t) fN, \tag{10}$$

where I_0 is the amount of insulin content in a granule, N is the total number of β-cells in the pancreas and $f(G)$ represents the fraction of total β-cell population which responds to the glucose stimulus and defined by the following relation as proposed in [20]

$$f(G) = \begin{cases} f_b, & G < G^* \\ f_b + (1 - f_b)\frac{G-G^*}{K_f+G-G^*}, & G \geq \hat{G} \end{cases} \tag{11}$$

where f_b is the fraction of responding β-cells at glucose concentration below the threshold G^* and K_f is the constant related to the effectiveness of β-cells requirement.

3. Analytical results

3.1. Positive invariance and boundedness

Result 1. (i) The interior $\mathbf{R}^7_+$ is invariant for system (9).
(ii) All solutions of the system (9) with positive initial conditions are uniformly bounded within a region Γ, where

$$\Gamma = \Big((M, P, R, \gamma, D, D_{IR}, \rho) \in \mathbf{R}^7_+ : \ 0 < M(t) \leq M_1, \ 0 < P(t) \leq P_1, 0 < R(t) \leq R_1,$$
$$l_1 \leq \gamma(t) \leq H_1, \ 0 < D(t) \leq D_1, \ 0 < D_{IR} < C_T, \ 0 < \rho(t) \leq H_2 \ \forall \ t \geq 0\Big),$$

with

$$M_1 = \frac{\alpha_1}{\delta_1} + M(0)$$
$$P_1 = \frac{\nu M_1}{\delta_2} + P(0),$$
$$l_1 = \gamma_b + \alpha_2,$$
$$H_1 = \gamma_b + \alpha_2 + \gamma(0),$$
$$H_2 = \Big(\rho_b + k_\rho(H_1 - \gamma_b)\Big) + \rho(0),$$
$$R_1 = \frac{kP_1C_TH_2}{l_1} + R(0),$$
$$D_1 = \frac{H_1R_1 + k_1^-C_T}{k_1^+\epsilon} + D(0).$$

Proof. see Appendix B. □

3.2. Equilibrium points and stability analysis

Result 2. The system (9) has
I. one non-interior equilibrium point,

$$E_{B0} \equiv (M_0^*, P_0^*, 0, \gamma_0^*, 0, 0, \rho_0^*) \tag{12}$$

which exists for all parameter values, where,

$$M_0^* = \frac{\alpha_1}{\delta_1},$$
$$P_0^* = \frac{\nu\alpha_1}{\delta_1\delta_2},$$
$$\gamma_0^* = \gamma_b + \alpha_2,$$
$$\rho_0^* = \rho_b + k_\rho\alpha_2.$$

II. one interior equilibrium point, namely

$$E^* \equiv (M^*, P^*, R^*, \gamma^*, D^*, D_{IR}^*, \rho^*), \tag{13}$$

where,

$$M^* = \frac{\alpha_1}{\delta_1},$$
$$P^* = \frac{1}{k},$$
$$R^* = \frac{k\nu\alpha_1 - \delta_1\delta_2}{k\delta_1(\gamma_b + \alpha_2)},$$

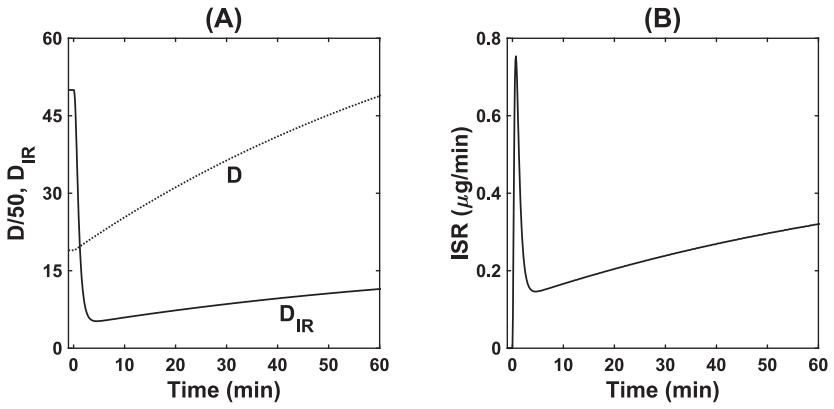

Fig. 2. Time evolution of the system (9) for G= 16.7 mmol/l. (A) the time course of D (dotted line) and D_{IR} (solid line) (B) time course of ISR. The time course was generated using the parameter value provided in Table 1 and satisfied the time series data given in [20] for the control condition.

$$\gamma^* = \gamma_b + \alpha_2,$$

$$D^* = \frac{(k\nu\alpha_1 - \delta_1\delta_2)(\rho_b + k_\rho\alpha_2 + k_1^-)}{k_1^+[C_T k\delta_1(\rho_b + k_\rho\alpha_2) - (k\nu\alpha_1 - \delta_1\delta_2)]},$$

$$D_{IR}^* = \frac{k\nu\alpha_1 - \delta_1\delta_2}{k\delta_1(\rho_b + k_\rho\alpha_2)}$$

$$\rho^* = \rho_b + k_\rho\alpha_2.$$

E^* exists if

(i) $(k\nu\alpha_1 - \delta_1\delta_2) > 0$ and
(ii) $C_T k\delta_1(\rho_b + k_\rho\alpha_2) > (k\nu\alpha_1 - \delta_1\delta_2)$.

E_{B0} will be locally asymptotically stable if $k\nu\alpha_1 < \delta_1\delta_2$. E^* will be locally asymptotically stable if

(i) $A\gamma^*\rho^* + AB\rho^* + BC\gamma^* > kAP^*\gamma^*\rho^*$,
(ii) $B > \delta_2 kP^*$,
(iii) $(B + C + \gamma^*)(A\rho^* + (B + C)\gamma^* + BC) > (A\gamma^*\rho^* - kAP^*\gamma^*\rho^* + AB\rho^* + BC\gamma^*)$,
(iv) $(B + C + \gamma^*)(A\rho^* + (B + C)\gamma^* + BC)(A\gamma^*\rho^* - kAP^*\gamma^*\rho^* + AB\rho^* + BC\gamma^*) >$
$(A\gamma^*\rho^* - kAP^*\gamma^*\rho^* + AB\rho^* + BC\gamma^*)^2 + (B + C + \gamma^*)^2(AB\gamma^*\rho^* - \delta_2 kAP^*\gamma^*\rho^*)$,

where, $A = k_1^+(C_T - D_{IR}^*)$, $B = (\delta_2 + k\rho^* D_{IR}^*)$ and $C = (A + k_1^+ D + k_1^- + \rho^*)$. If all of these conditions are satisfied then E^* will be globally asymptotically stable, since according to the existence criterion of E^*, E_{B0} will be unstable.

Proof. see Appendix C. □

4. Numerical results

We begin the analysis assuming that the system remains in the steady state (i.e., in interior equilibrium point, E^*) at low glucose concentration, and the high glucose concentration would act as a stimulus. To capture the effect of glucose stimulus on the system, two threshold values of glucose, G^*= 4.58 mmol/l and $\hat{G}$= 10 mmol/l, were used. Based on this values, we obtained α_2=0 for low glucose setting ($G \leq$ 4.58 mmol/l) and $\alpha_2 = \hat{h} = 3.93 \times 10^{-3}$ min^{-1} for high glucose setting ($G \geq$ 10 mmol/l). The rest of the parameters were collected or derived from the information given in available literature (detailed descriptions are provided in Table 1 and Appendix A). The collected parameters are from the rat pancreas. The values of ν and k were estimated such that for low glucose, the system (9) provides the stable interior equilibrium point (E^*), where M^*=126753, P^*=10, R^*=10,000, D^*=950, D_{IR}^*=50, $\gamma^* = \gamma_b$ and $\rho^* = \rho_b$ [20,30]. It is well-known that high glucose levels in β-cells increase the translation rate of the insulin gene [15]. So, we also increased the value of ν for the high glucose model simulation. ν was estimated by reproducing the time series data (Fig. 2) given in [20]. The pattern of insulin secretion rate (ISR) in response to the glucose stimulation for glucose concentration of 16.7 mmol/l (300 mg/100 ml) was well matched with the experimental data provided for the perfused rat pancreas [31]. The obtained parameter set (given in Table 1) for the high glucose model stimulation also satisfies the existence and stability criterion for the interior equilibrium of the system (9).

Table 1
Description of the parameters: Values of the parameters were mostly collected from the available literature. For some unknown parameters, we estimated their values by using the available information literature, and detailed descriptions were provided in Appendix A.

Parameters	Definition	Value with unit	Ref.
α_1	Transcription rate constant	50.4934 tpm min^{-1} (low glucose), 116.89 tpm min^{-1} (high glucose)	Estimated
δ_1	mRNA degradation rate constant	3.98×10^{-4} min^{-1} (low glucose), 1.5×10^{-4} min^{-1} (high glucose)	Estimated
υ	Biosynthesis rate constant of proinsulin aggregates from insulin mRNA	3.16×10^{-5} tpm^{-1} min^{-1} (low glucose), 7.89×10^{-5} tpm^{-1} min^{-1} (high glucose)	Estimated
δ_2	Degradation rate constant of proinsulin pool	0.3 min^{-1}	[20]
k	Rate constant of formation of insulin granules	0.1	Estimated
η	Rate constant for γ	4 min^{-1}	[20]
γ_b	Basal value of γ at low glucose	10^{-4} min^{-1}	[20]
$\hat{h}$	Maximal value of glucose-stimulated γ input rate	3.93×10^{-3} min^{-1}	[20]
k_1^+	Association rate constant for the binding between granule and Ca^{2+} channels	1.447×10^{-5} min^{-1}	[20]
C_T	Constant pool of total Ca^{2+} channels	500	[23]
k_1^-	Dissociation rate constant for the binding between granule and Ca^{2+} channels	0.10375 min^{-1}	[20]
ζ	Rate constant for ρ	4 min^{-1}	[20]
ρ_b	Basal value of ρ at low glucose	0.02 min^{-1}	[20]
k_ρ	Sensitivity of ρ on the activatory action of γ	350	[20]
I_0	Amount of insulin content in a granule	1.6 amol	[24]
f_b	Fraction of responding β-cells at glucose concentration below the threshold G^*	0.05	[20]
K_f	Constant related to the effectiveness of β-cells requirement	3.43 mmol/l	[20]
N	Total number of β-cells	2.76×10^6	[25]

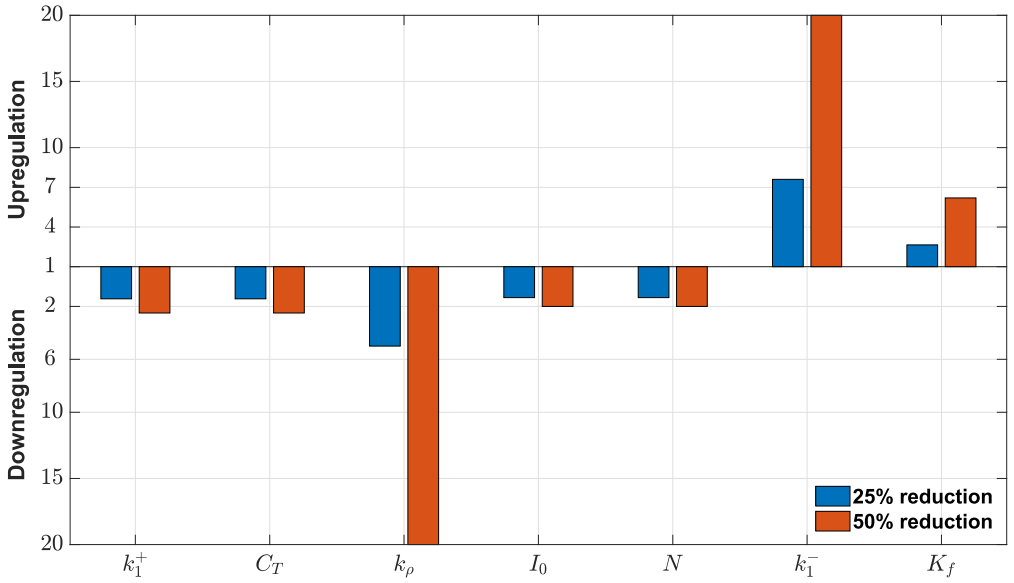

Fig. 3. Parameters that are affected by impaired pancreatic β-cells in T2D. The length of the bar graph denotes the amount of perturbation (in fold change) in different parameters due to impaired insulin secretion. When the insulin secretion is reduced by 25% from the normal level, the bar representing the parameter perturbation is plotted in blue color, while the orange color bar represents the effect on parameter perturbation due to a 50% reduction. (For interpretation of the references to colour in this figure legend, the reader is referred to the web version of this article.)

Type 2 diabetes (T2D) is characterized by diminished or inadequate insulin secretion from β-cells, which could be a defect of either β-cell function or loss of β-cell mass [32,33]. It was reported that glucose-stimulated insulin secretion (GSIS) in T2D islets averaged $\sim$ 75% of control islets, which means $\sim$ 25% reduction in insulin secretion [34]. Here, we simulated the model to capture the effect of impaired pancreatic β-cells on different parameters to see how they are perturbed in disease conditions. We obtained seven parameters perturbed in the impaired pancreatic β-cells in T2D (Fig. 3). These parameters are the alterations in the GSIS process (k_1^+, C_T, k_1^- and k_ρ), loss in β-cell mass (N), reduced insulin content in the insulin granules (I_0), and diminished response of β-cells in glucose stimulus (K_f). Among them, the ATP-dependent calcium influx (k_ρ) significantly reduces in the impaired pancreatic β-cells, while the dissociation of the calcium channels from the insulin

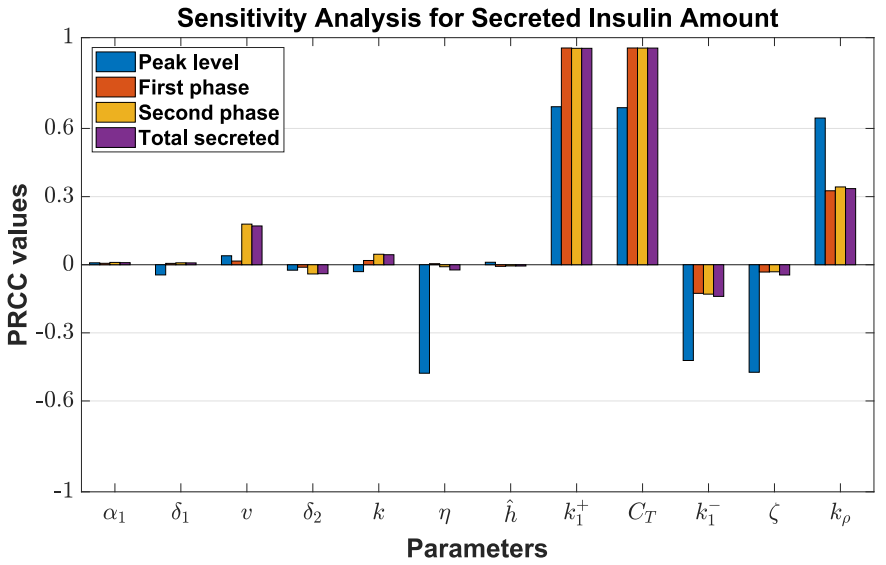

Fig. 4. Global sensitivity analysis for glucose-stimulated insulin secretion rate (*ISR*). This was performed by using Latin Hypercube Sampling (LHS) and Partial Ranked Correlation Coefficient (PRCC) technique [35] under high glucose situation. Here, the peak level denotes the highest value in the ISR, the first phase indicates the cumulative sum of ISR within the time interval of 0–8 min, the second phase represents the cumulative sum of ISR within the time interval of 9–120 min, and the sum of the first and second phases represents the total secreted amount of insulin. The length of each bar represents the sensitivity of each parameter on the output (given in figure legend). Sensitive parameters were selected based on the threshold value ± 0.3 on PRCC value [17,36].

granules (k_1^-) shows a significant increase. So the model simulation shows a relation between impaired pancreatic β-cells and different parameter perturbations in T2D. Thus to get an insight into these relations, we performed an extensive model simulation with different parameter variations and identified crucial parameters that significantly affect insulin secretion from β-cells under high or low-glucose conditions. This would help to understand the pathophysiology of T2D as well as insulinoma.

4.1. Factors responsible for reduction in glucose-stimulated insulin secretion

Global sensitivity analysis (GSA) was performed to get an initial picture of the crucial parameters responsible for reducing insulin secretion under a high glucose medium. The simulations were performed for the time interval 0–120 min. The initial value for the simulation was taken from the literature [20,30] representing the basal of the variables. We sought to identify parameters that hampered insulin secretion in T2D patients and focused only on the insulin secretion rate (*ISR*). The highest value in the insulin secretion rate within this time interval was considered as the peak level (Fig. 2B). The first phase of insulin secretion was denoted by the amount of insulin secreted within 0–8 min. The second phase of insulin secretion was represented by the amount of insulin secreted within 9–120 min. The total secreted amount was calculated by taking the sum of the first and second phases of insulin secretion. Here, we used Latin Hypercube Sampling (LHS) and Partial Ranked Correlation Coefficient (PRCC) technique for the GSA and the sensitivity of the parameters was captured for these four outputs. In this analysis, each of the parameters was uniformly varied by using the LHS method over a range of ± 2-folds from their defined values given in Table 1 for 1000 number of simulations. Then, the model system (9) was simulated using each combination of parameter values and the model output of interest was collected. Finally, correlations between the input parameters and the output variables were calculated using the PRCC method [35,37], which varies between $+1$ (perfect positive association/correlation) and -1 (perfect negative association/correlation). Parameters with an absolute PRCC value greater than 0.3 were considered sensitive parameters [17,36]. Here, six system parameters (η, $k_1{}^+$, C_T, $k_1{}^-$, ζ and k_ρ) were obtained sensitive to insulin secretion (Fig. 4) and were associated with insulin granules trafficking and the exocytosis processes. Among them, η, $k_1{}^-$ and ζ were only sensitive to peak insulin secretion rate, and the other three were sensitive for all four outputs. To uncover the effect of these parameters on the loss of insulin secretion in glucose stimulus, we varied them 5-fold up-and-down from their default values (provided in Table 1). Down-regulation of $k_1{}^+$, C_T and k_ρ, and up-regulation of $k_1{}^-$ from their baseline values resulted in reduced first-and second-phase insulin secretion (Fig. 5). Altered values of $k_1{}^+$, $k_1{}^-$ and C_T reflect the defects in the formation of immediately releasable granules from the docked granules due to loss in the level of Ca^{2+} channels or any impairment in binding with insulin granules. Impairment in the value of k_ρ represents the defects in the activatory action of ATP on intracellular Ca^{2+} contents, which can be caused due to overactivity of the K_{ATP} channels. Additionally, we observed that reducing the value of η and ζ could only diminish the value of the peak insulin secretion rate. Any impairment of their values represents the defects in the proper rise in the ATP-to-ADP ratio and cytosolic Ca^{2+} concentration in response to the glucose stimulus, respectively.

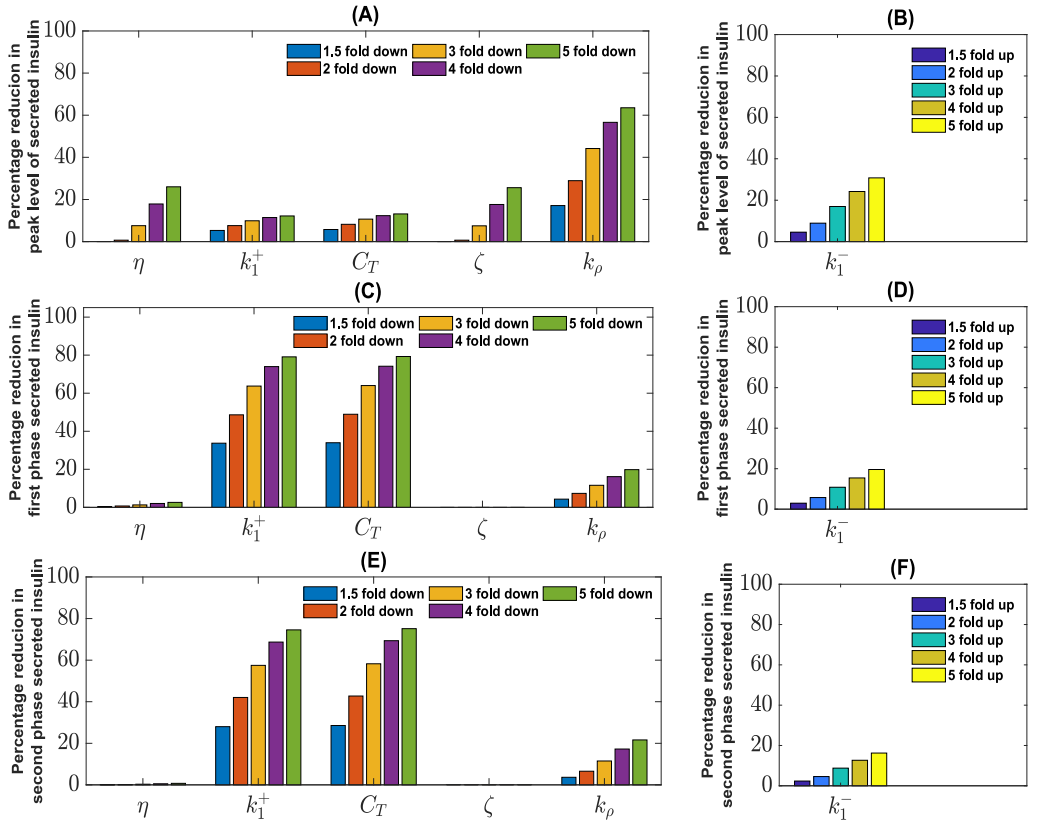

Fig. 5. Effect of sensitive parameters on glucose-stimulated insulin secretion rate. We classified the findings into two categories: one is where down-regulation of the parameters reduces insulin secretion (first column), and another one is where up-regulation reduces insulin secretion (second column). Each of these parameters was varied up to 5-fold, and subsequently, the reductions in the values of peak insulin secretion rate (first row) and amount of secreted insulin in the first (second row) and second (third row) phases were observed.

From the stability analysis of the system (9), we observed that parameters related to the insulin synthesis process have a vital role in the existence of an axial equilibrium point (E_{B0}). Still, their effects were not observed here in the simulations within 0–120 min intervals. The most likely explanation is that their variations had no discernible impact on the level of proinsulin aggregates during these periods. We also observed that changes to the transcription and mRNA stability-associated parameters could not affect the insulin mRNA expression level within this short period. People with insulin resistance experience high glucose for longer than normal individuals after taking the food. So, an important question is whether the changes in those parameters can affect the systems in a longer time frame. It is reported that chronic hyperglycemia decreases insulin mRNA expression by reducing promoter activity and downregulating the expression of two important transcription factors of insulin [22]. So, exploring the effect of transcription, mRNA stability, and translation-associated parameters on the insulin secretion rate could help us understand the impact of reduced insulin synthesis on the pathophysiology of T2D. Here, we obtained three parameters that are associated with the transcription rate of the insulin gene (α_1), stability of the insulin mRNA (δ_1), and translation rate from the insulin mRNA (ν). So, we varied these three parameters individually and synergistically in the system for the time interval 0–24 hrs and captured the insulin secretion rate. It was found that reduction in α_1 and ν, and increment in δ_1 causes a marked reduction in the insulin secretion rate at the final time point (Fig. 6). Among them, the impact of the reduction in ν is much more than the others. This represents the reduced biosynthesis rate of proinsulin aggregates from inulin mRNA and might be caused due to defects in the translation and post-translational modification processes. Reduction in α_1 and increment in δ_1 causes reduced insulin secretion by reducing insulin mRNA level and represents the defects in the transcription and mRNA stability, respectively.

In our study, the insulin secretion rate is a function of the pool of immediately releasable insulin granules (D_{IR}), so it is also interesting to understand the parameters responsible for the existence of the stable axial equilibrium point E_{B0} (12) in high glucose situations. It would capture the molecular mechanisms behind the loss of insulin secretion from β-cells under high glucose concentrations. To capture the significance of the parameters, we varied each of them from zero to a value that is 10-fold higher than the default value. It was observed that E_{B0} would be stable if any of the three parameters α_1, ν, and k become zero. These three are associated with insulin's transcription and translation processes and the formation of insulin granules. The two-dimensional parameter variation captures the possible ranges for the stability of E_{B0} (Fig. 7). We obtained

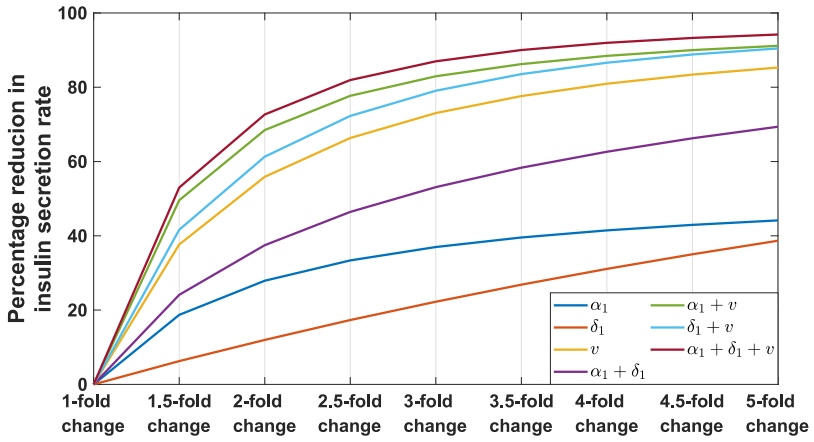

Fig. 6. Effect of transcription, mRNA stability and translation-associated parameters on glucose-stimulated insulin secretion rate. To mimic the reduction in transcription and translation rate, here we decreased the value of α_1 and v, respectively, whereas the reduced mRNA stability rate was imposed by increasing the value of δ_1. All the simulations were performed for the time interval of 0–24 hrs and the effect of parameter variations was captured at the final time point.

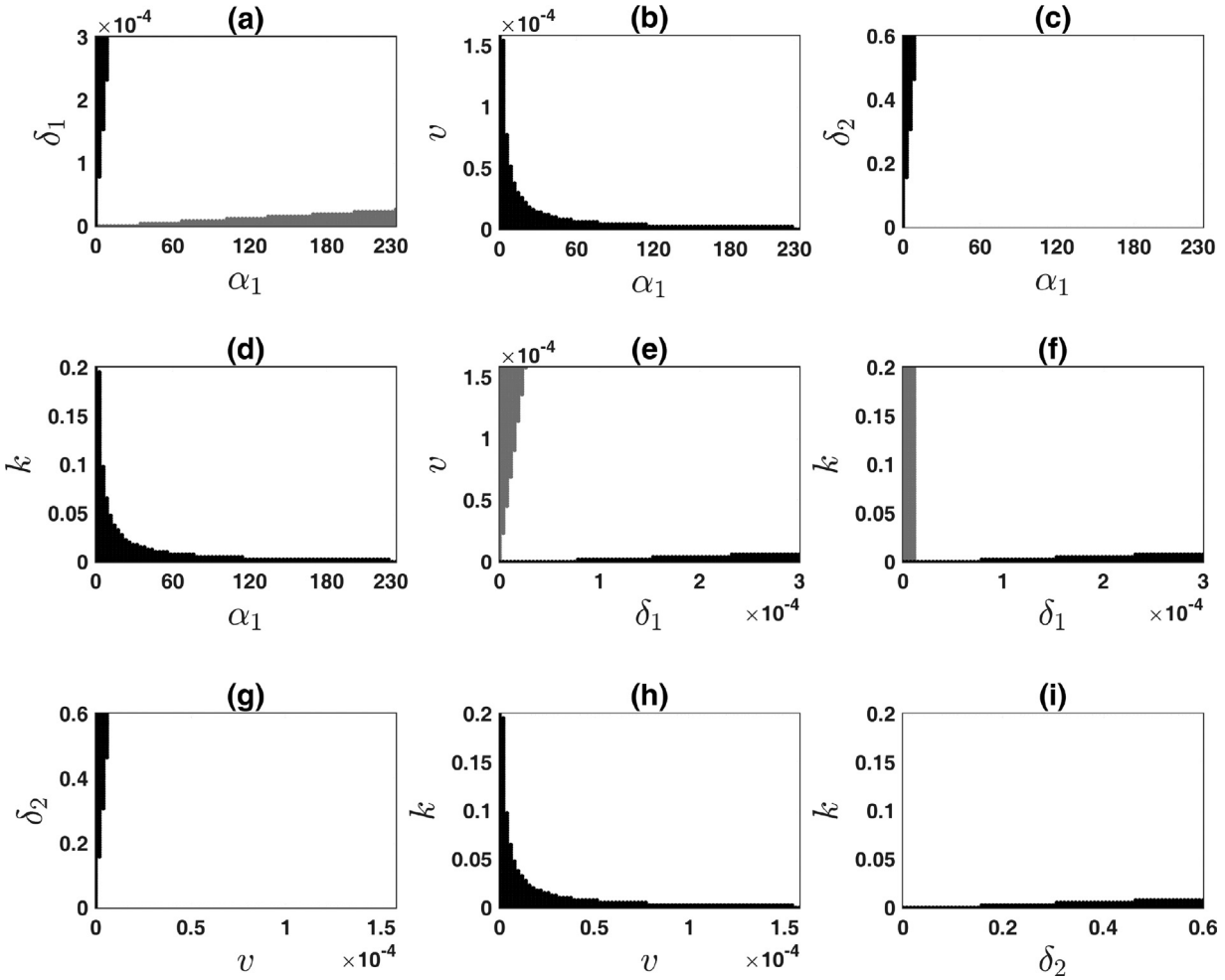

Fig. 7. Two-dimensional parameter space representing the nature of the equilibrium point for the system (9). In the white-colored region, the system has one stable interior equilibrium point (E^*) and one unstable axial equilibrium point (E_{B0}). In the grey-colored region, condition (ii) for the existence of E^* is not satisfied. In the black-colored region, condition (i) for the existence of E^* is not satisfied and the axial equilibrium point (E_{B0}) becomes stable.

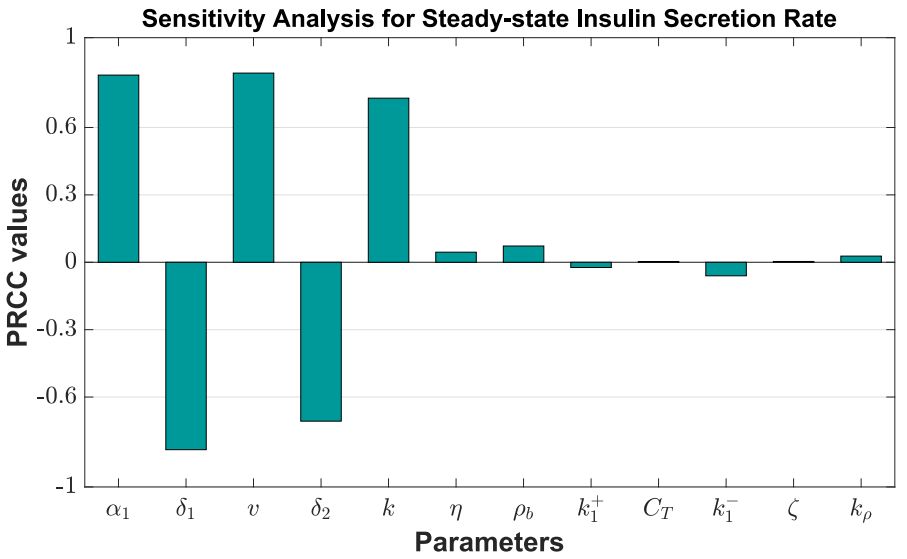

Fig. 8. Global sensitivity analysis for the insulin secretion rate at the steady state of the system. This was performed by using Latin Hypercube Sampling (LHS) and Partial Ranked Correlation Coefficient (PRCC) technique [35] under low glucose situation. The length of each bar represents the sensitivity of each parameter to the value of insulin secretion rate at the interior equilibrium point (E^*). Sensitive parameters were selected based on the threshold value ± 0.3 on PRCC value [17,36].

two additional parameters (δ_1 and δ_2) whose imbalance with the above three parameters made the axial equilibrium point stable. However, the 2D parameter analysis shows the dominance of the former three over the later two in maintaining the stable axial point. Our analysis also highlighted that decreased values of the former three parameters and the elevated values of the latter two could be the possible causes for the loss of insulin secretion from β-cell. It is noteworthy that all of these primarily reflect the defects in insulin synthesis and the formation of insulin granules.

Hence, the reduced insulin synthesis rate and defects in granule exocytosis processes cause reduced insulin secretion from β-cells. The latter has an immediate effect and can hamper first- and second-phase insulin secretion, whereas the former lowers the insulin secretions after a long period and can cause a complete loss of insulin. We were now focused on identifying parameters that can cause elevated insulin secretion from β-cell under the low glucose condition to understand the mechanisms behind hyperinsulinemia.

4.2. Uncontrolled insulin secretion under low glucose

The insulinoma cell, a rare neuroendocrine pancreatic tumour cell, secretes insulin at low blood glucose [6]. So, all insulinoma patients experience hyperinsulinemic hypoglycemia [38]. Understanding the pathophysiology of insulinoma requires identifying the factors responsible for the elevated insulin secretion from β-cell under the low glucose condition. We assumed the system would always stay at the basal level (i.e., in a steady state) in low glucose concentration. The simulations focus on identifying parameters affecting the basal insulin secretion rate at low glucose settings. To get the basal insulin secretion rate, we calculated the interior equilibrium (E^*) point for each parameter set, and then Eq. (10) was used. GSA provided five system parameters (α_1, δ_1, v, δ_2 and k) sensitive to the basal insulin secretion rate (Fig. 8). Hence, we concentrated on these parameters for further exploration. Each of these parameters was varied 5-fold up-and down from their default values (provided in Table 1), and subsequently, the increment in the steady-state insulin secretion rate was observed. Up-regulation of α_1, v and k, and down-regulation of δ_1 and δ_2 resulted in elevated steady-state insulin secretion rate (Fig. 9). Interestingly, none of them are associated with the insulin granules trafficking and exocytosis processes but rather reflect the uncontrolled insulin synthesis inside the β-cell.

4.3. Insulin synthesis and exocytosis processes in managing the insulin secretion dynamics

It was observed that the reduced insulin synthesis rate and defects in granule exocytosis processes cause reduced insulin secretion from β-cells. The latter has an immediate effect and the former act after a long period. However, it was observed that only the small perturbations in the parameters related to insulin synthesis processes were compensated by the parameters associated with insulin granule trafficking and exocytosis (Fig. 10). For example, up to 0.7-fold changes in transcription rate (α_1), 3-fold changes in mRNA degradation rate (δ_1), and 0.6-fold changes in insulin granules formation rate (k) was fully compensated, but it requires almost 10-fold changes in tuning parameters. In contrast, the parameters related to insulin synthesis showed better restoration capability in case of reduced insulin secretion due to defective insulin

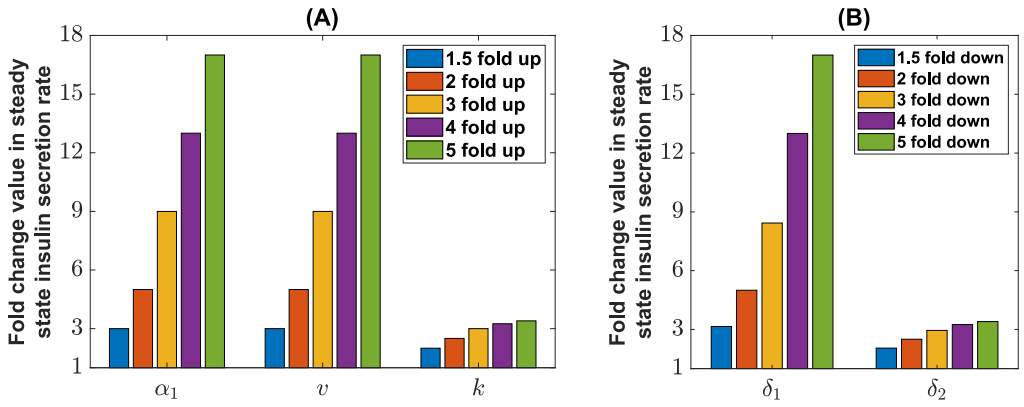

Fig. 9. Effect of sensitive parameters on insulin secretion rate at the low glucose concentration. We classified the findings into two categories: one is where the up-regulation of the parameters increases insulin secretion (A), and another one is where the down-regulation increases insulin secretion (B). Each of these parameters was varied up to 5-fold, and subsequently, the increment in the insulin secretion rate was observed. Each of these parameters was varied up to 5-fold, and subsequently, the increment in the steady state insulin secretion rate was observed because we assumed that the system would stay in a steady state at low glucose concentration.

granule trafficking and exocytosis (Fig. 11). Up-regulation of transcription (α_1) and translation (v) rates were found as the most effective strategies for restoring insulin secretion during impaired insulin granule trafficking and exocytosis.

We already established that increased insulin synthesis could cause uncontrolled insulin secretion from pancreatic β-cells during the non-diabetic state. However, single parameter variation related to the insulin granules trafficking and exocytosis processes showed no effect in restoring increased basal insulin secretion from β-cells (Fig. 12).

4.4. Restoration strategies for compensating the β-cells mass

The amount of insulin released from the pancreas is mainly determined by the product of the β-cells functional mass and the insulin secreted by each cell. So, the body requires an appropriate number of insulin-secreting β-cells to maintain homeostasis. T2D is a complex metabolic disorder in which chronically increased glucose levels causes the loss of β-cell mass by promoting cell death or dedifferentiation [22,39–41]. Hence, we focused on identifying possible restoration strategies for compensating the β-cell mass by tuning different systems parameters. Our analysis revealed that regulation of the transcription (α_1) and translation (v) have a significant impact on restoring insulin secretion (Fig. 13). Besides, δ_1, δ_2, k, ${k_1}^+$ and C_T had very minor effect.

When β-cell mass increases due to a tumor inside the pancreatic islet (like in insulinoma patients), insulin secretion also increases [42]. In this context, reducing the basal insulin secretion rate would be beneficial to control fasting hypoglycemia. We tuned each system parameter to control the basal insulin secretion rate for different β-cell numbers. Only three parameters (α_1, v and k) were obtained as possible restoration candidates (Fig. 14). These mainly reflect the reduction of the insulin synthesis through the tuning of transcription (α_1) and translation (v) and the downregulation of insulin granules formation rate (k).

5. Discussion

Insulin is an endocrine peptide hormone secreted from pancreatic β-cells that plays an essential role in maintaining glucose homeostasis in our body. Its secretion from β-cells in response to the glucose stimulus is mainly biphasic [8–10]. Glucose also regulates insulin synthesis by controlling various processes, including the proinsulin gene transcription, mRNA stability, and the translational process [10,13]. The glucose-insulin relationship gets affected under various pathophysiological conditions like insulinoma [6]. Numerous studies have been performed to comprehend this complex dynamical process. However, the mechanisms regulating glucose-stimulated insulin synthesis and secretion under physiological and pathophysiological conditions are not clear [5]. This motivates us to investigate the potential causes that change insulin secretion with different glucose conditions. The current study proposed and analyzed a minimal model involving insulin synthesis, and secretion processes. It identifies crucial factors whose abnormalities could lead to either Type 2 diabetes (T2D) or hyperinsulinemic hypoglycemia. Here, we included the insulin mRNA level as a variable in the model to investigate the consequences of defects in the transcription and translation processes of the insulin gene. We first studied the model analytically and identified the existence and stability conditions for the interior (E^*) and axial (E_{B0}, absence of insulin granules) equilibrium points. We found that the stability of E_{B0} depends on five parameters satisfying the inequality $kv\alpha_1 < \delta_1\delta_2$. The parameter set acquired for the numerical simulations satisfies the stability conditions for the interior steady state as well as the normal physiology of the system. We varied these parameters to obtain different conditions correlating with various pathophysiological conditions.

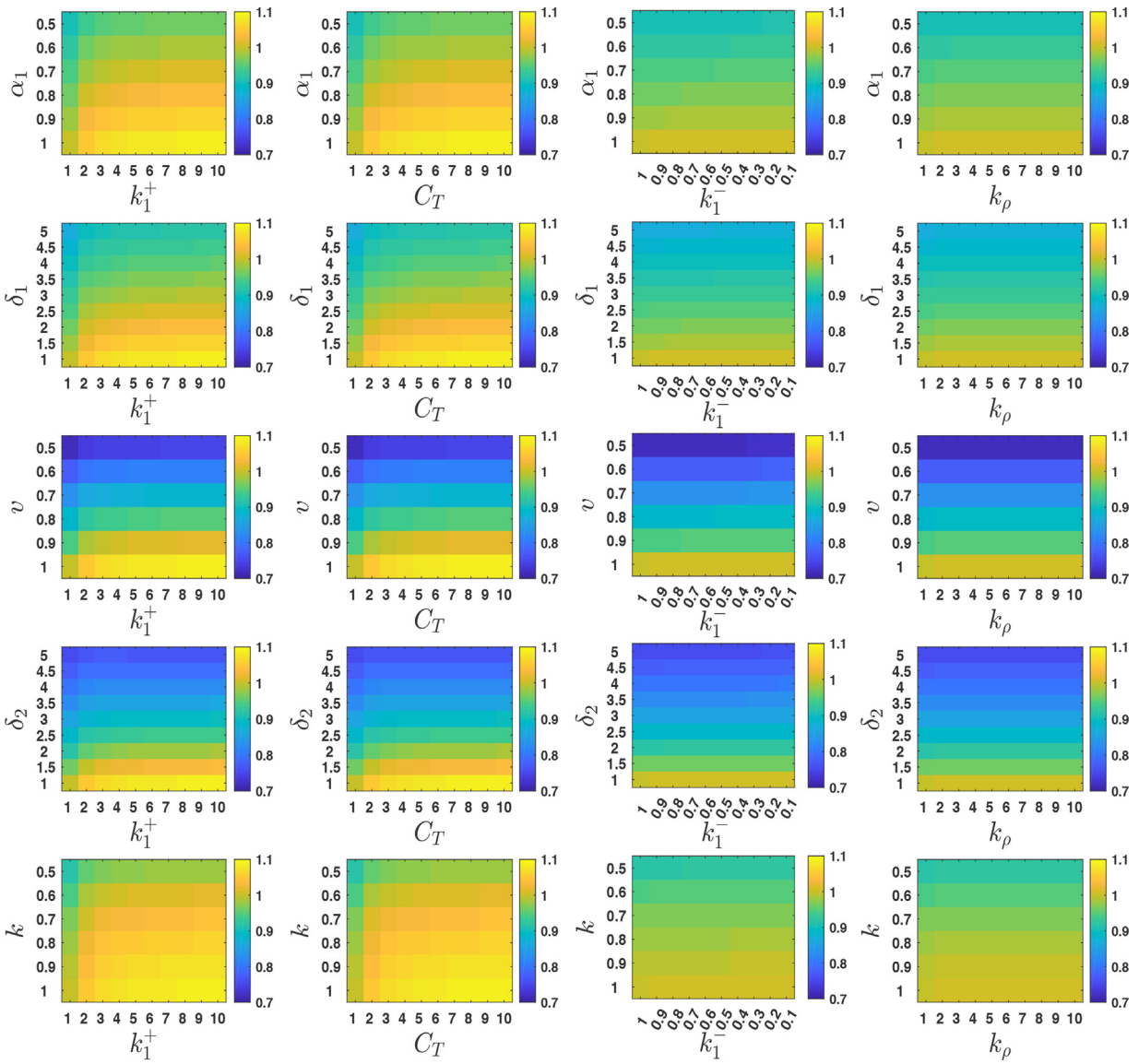

Fig. 10. Tuning effect of the parameters related to the insulin granule trafficking and exocytosis processes in compensating insulin secretion due to decreased insulin synthesis inside the β-cell. Here the vertical axes denote the fold changes for those parameters for which the restoration was performed. In contrast, the horizontal axes represent the fold changes for the parameters by which the tuning was made. The color bar represents the fold change value in the total secreted insulin level compared to the default parameters for the high glucose model simulation. In all of these cases, simulations were performed for the time interval 0–24 hrs. (For interpretation of the references to colour in this figure legend, the reader is referred to the web version of this article.)

β-cell dysfunctioning plays a crucial role in the initial stages of T2D development and persists as the disease progresses [43]. We seek parameters that could hamper the insulin secretion rate. The parameter variation analysis identified four parameters responsible for reducing first (0–8 min) and second-phase (9–120 min) insulin secretion rates and two parameters responsible for the diminished value in the peak insulin secretion rate. These highlight the two major areas of insulin granules trafficking and secretory processes. They are 1) defects in forming immediately releasable granules from the docked granules and 2) defects in the glucose-evoked rise in intracellular Ca^{2+} content. Our analysis suggests that immediately releasable granule formation could be hampered due to a decreased level in Ca^{2+} channels or any impairment in its binding with insulin granules. On the other hand, overactivity of the K_{ATP} channels and improper rise in the ATP-to-ADP ratio in response to the glucose stimulus could also hamper the glucose-evoked rise in intracellular Ca^{2+}. It has been observed in the literature that polymorphism of the K_{ATP} channel (E23K) could also be a risk factor for T2D [44]. It is also reported that activating mutations in Kir6.2 and sulfonylurea receptor 1 (SUR1) subunits of the K_{ATP} channel are the major causes of neonatal diabetes [44]. The above shorter time frame (0–120 min) simulation did not capture the effect of decreased insulin

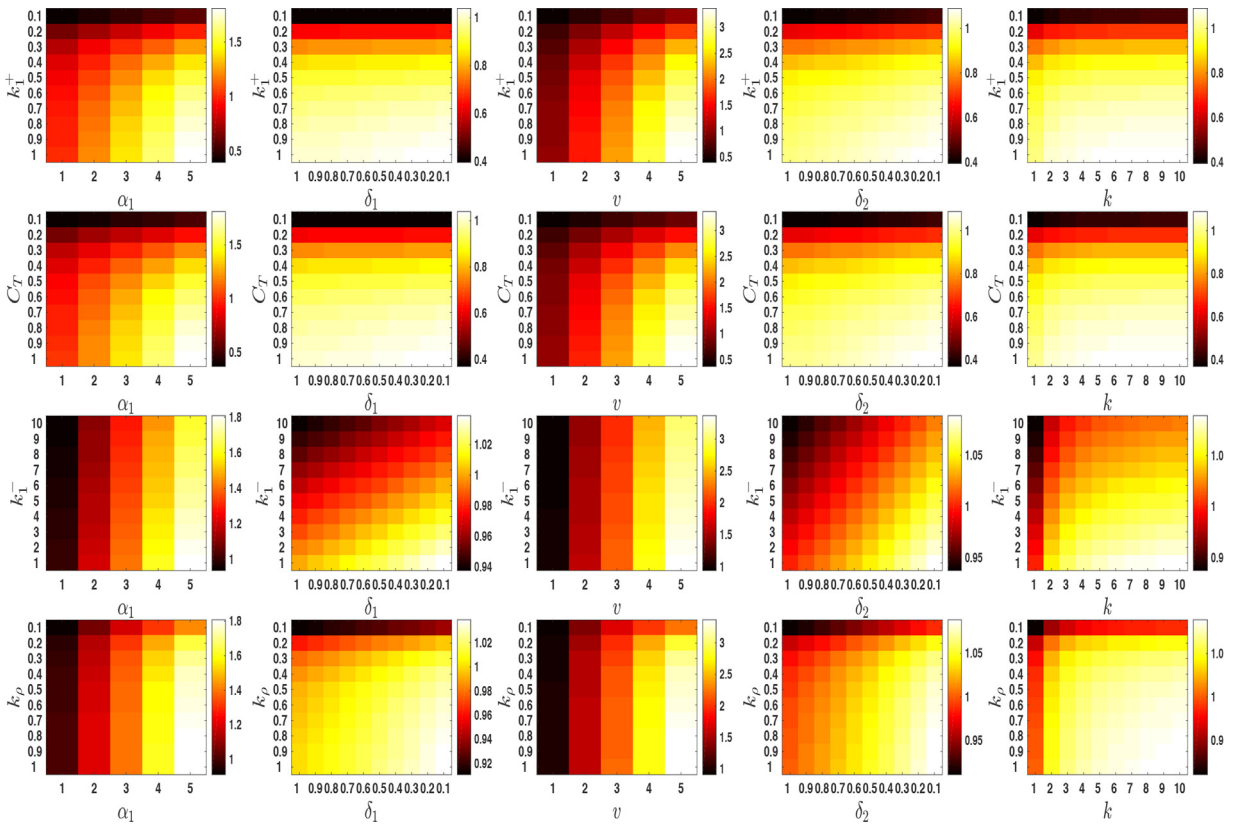

Fig. 11. This figure depicts the tuning effect of the parameters related to insulin synthesis for reversing reduced insulin secretion due to defective insulin granule trafficking and exocytosis. Here the vertical axes denote the fold changes for those parameters for which the restoration was performed. In contrast, the horizontal axes represent the fold changes for the parameters by which the tuning was made. The color bar represents the fold change value in the total secreted insulin level compared to the default parameters for the high glucose model simulation. In all of these cases, simulations were performed for the time interval 0–24 hrs. (For interpretation of the references to colour in this figure legend, the reader is referred to the web version of this article.)

synthesis rate on insulin secretion. However, the impact was observed in a longer time frame (0–24 hrs) simulation, which showed that reduced insulin synthesis rates could hamper insulin secretion.

We observed that the pancreatic β-cells could become empty with respect to insulin granules (i.e., E_{B0} becomes stable) due to combined reductions of any two processes: transcription, translation, and insulin granules formulation rates. Besides, an increased degradation rate of insulin mRNA or proinsulin pool, along with reductions in any of the above mentions three processes, could cause the same. However, the former three are more dominant over the latter two in causing loss of insulin content inside the β-cells. Literature suggests that metabolic stress due to the chronic oversupply of nutrients could lead to reduced expression or activity of critical β-cell transcription factors, including FOXO1, PDX1, NKX6.1, and MAFA [45–48]. Subsequently, some crucial end-differentiated genes, including insulin itself, were lost [49], causing depletion in insulin synthesis. So, defects in the insulin synthesis and the insulin granules formation processes might contribute to the complete loss of insulin inside the β-cells during T2D development.

The present study also focuses on identifying parameters that elevate insulin secretion from the pancreas during the non-diabetic state. The investigation highlights the specific biological processes whose impairment might cause hyperinsulinemic hypoglycemia. The insulin secretion rate is a function of several factors, including the number of granules that undergo exocytosis, insulin content in each granule, β-cell mass, and the fraction of cells responding to the glucose stimulus. So, it is evident that an increase in their value might lead to excess insulin secretion from the pancreas. Apart from these factors, we obtained five additional system parameters that might cause abnormalities in the β-cells ability to adequately suppress insulin release in the presence of low circulating glucose. Thus, we might conclude that the up-regulation of insulin granule formation due to elevated transcription rate, increased mRNA stability, elevated translation rate, or reduced degradation rate of the proinsulin pool could cause hyperinsulinemic hypoglycemia. Although the insulin secretion rate depends on the number of granules undergoing exocytosis, we didn't find any impact of the parameters associated with the insulin granules trafficking and exocytosis processes on causing increased basal insulin secretion rate. Instead, our results suggest that the uncontrolled insulin synthesis inside the β-cell or the increased β-cell mass could be the major reasons for fasting hypoglycemia in insulinoma patients.

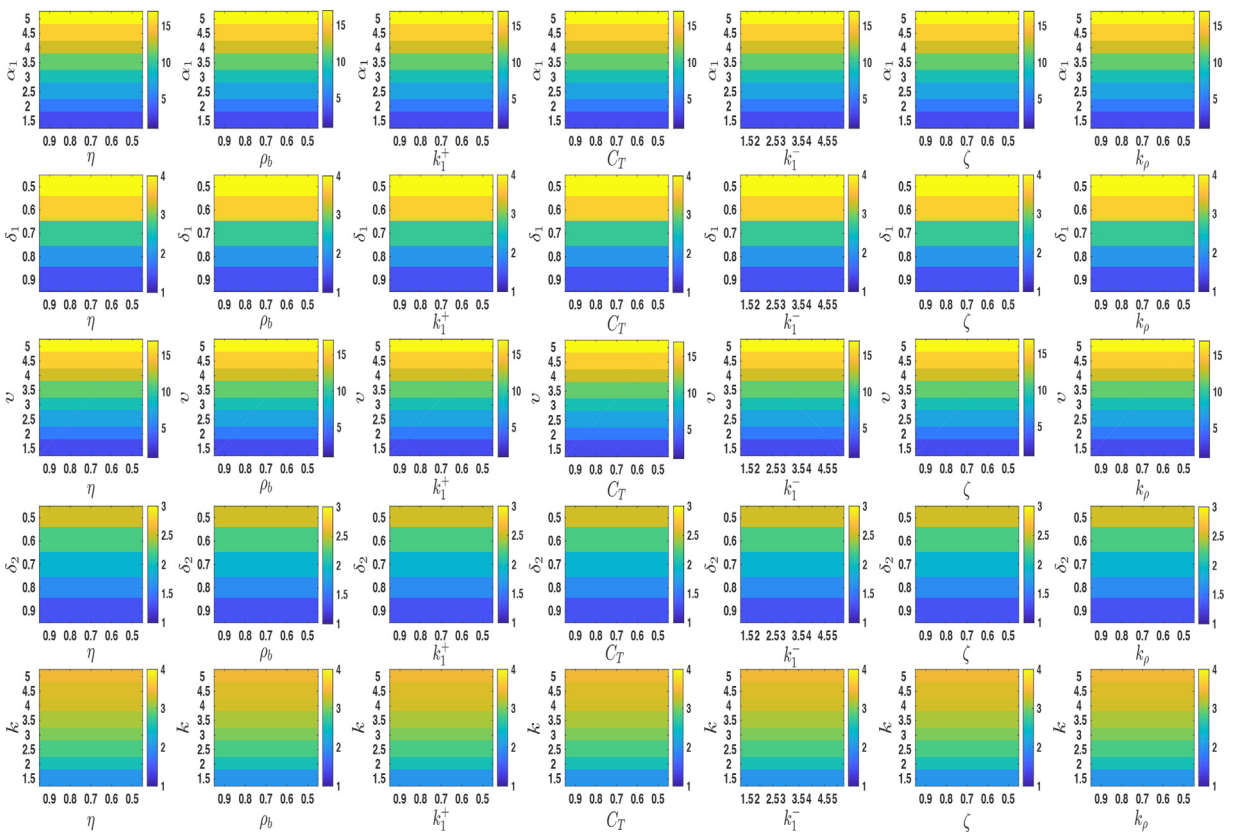

Fig. 12. This figure depicts the tuning effect of the parameters related to insulin granule trafficking and exocytosis processes for reversing uncontrolled insulin secretion due to upregulated insulin synthesis inside the β-cell. Here the vertical axes denote the fold changes for those parameters for which the restoration was performed. In contrast, the horizontal axes represent the fold changes for the parameters by which the tuning was made. The color bar represents the fold change value in the steady-state insulin secretion rate compared to the default parameters for the low glucose model simulation. (For interpretation of the references to colour in this figure legend, the reader is referred to the web version of this article.)

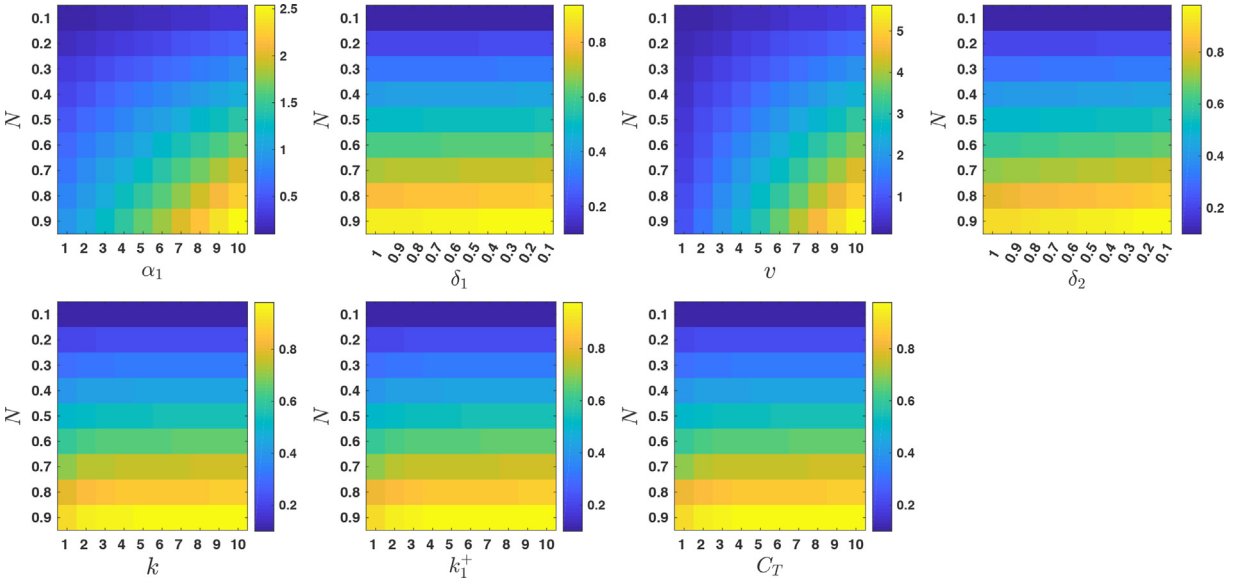

Fig. 13. This figure depicts the tuning effect of the parameters related to insulin synthesis and secretion processes for reversing reduced insulin secretion due to loss of β-cell mass. Here the vertical axes denote the fold changes for the parameter representing the β-cell mass. In contrast, the horizontal axes represent the fold changes for the parameters by which the tuning was made. The color bar represents the fold change value in the total secreted insulin level compared to the default parameters for the high glucose model simulation. In all of these cases, simulations were performed for the time interval 0–24 hrs. (For interpretation of the references to colour in this figure legend, the reader is referred to the web version of this article.)

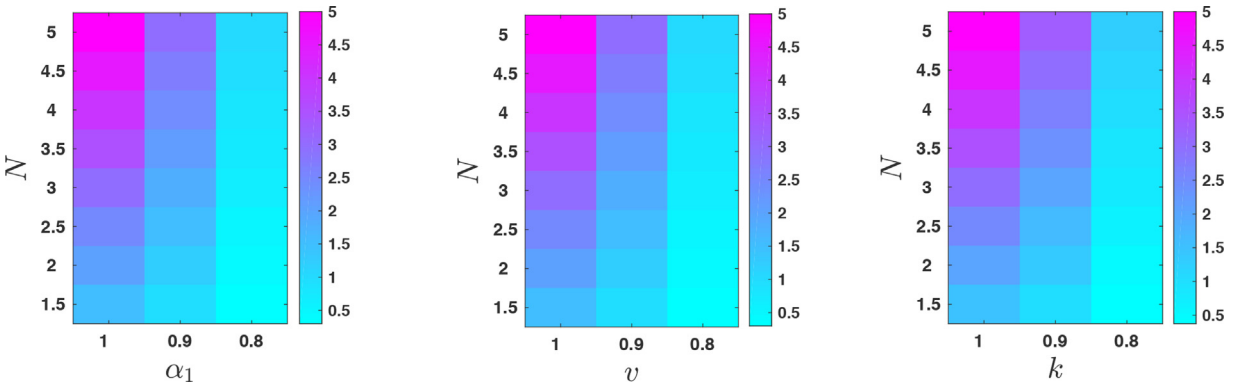

Fig. 14. This figure depicts the tuning effect of the parameters related to insulin synthesis for controlling insulin secretion due to increased β-cell mass. Here the vertical axes denote the fold changes for the parameter representing the β-cell mass. In contrast, the horizontal axes represent the fold changes for the parameters by which the tuning was made. The color bar represents the fold change value in the steady-state insulin secretion rate compared to the default parameters for the low glucose model simulation. (For interpretation of the references to colour in this figure legend, the reader is referred to the web version of this article.)

Our analyses revealed that alterations in the insulin synthesis and granule formation processes are difficult to manage by tuning parameters related to granule trafficking and exocytosis. Although these parameters could restore impaired insulin secretion due to a slight reduction in insulin synthesis, it requires almost 10-fold perturbation. Even beyond a certain level, increasing the rate of granule exocytosis cannot compensate for the decreased insulin synthesis. It also seems reasonable, as any defects in the insulin synthesis process, either by transcription or translation, ultimately affect the flux from the proinsulin pool to the immediately releasable granules pool. Subsequently, the exocytosis rate might get hampered due to the loss of insulin granules inside the β-cell. Hence, only the regulation of granules trafficking and exocytosis processes might fail to compensate for the impaired insulin synthesis. On the other hand, the accelerating insulin synthesis might restore the decreased insulin secretion driven by defective insulin granule trafficking and exocytosis processes. It can also potentially restore insulin secretion from the pancreas in the case of significant loss in β-cell mass. Thus, rather than only targeting the insulin secretion process, we need to target insulin synthesis and secretion both in managing T2D. Recently, several GLP-1 receptor agonists have been approved in the United States for the treatment of T2D, which have beneficial effects on both insulin synthesis and insulin secretion [50,51]. These increase insulin synthesis by targeting the transcription of insulin. However, we found that transcriptional regulation also has good restoration capabilities; hence, it might give new directions toward T2D management. In the case of insulinoma patients, our analysis suggests that targeting insulin synthesis by reducing transcription or translation could become a potential therapeutic strategy for controlling hyperinsulinemic hypoglycemia. This will reduce the insulin secretion from β-cells and also have the potential to compensate for the increased β-cell proliferation, as observed in insulinoma tumours.

Our study unveiled the importance of targeting insulin synthesis (transcription and translation) for controlling impaired insulin secretion. However, the present study is limited by the fact that we considered a constant transcription rate (α_1) in the equation $\frac{dM}{dt}$ and the proinsulin pool's biosynthesis rate (vM) as a linear function of M in the equation $\frac{dP}{dt}$. These two processes are very complex; for example, the transcription rate of the insulin gene is regulated by complex interactions between the transcription factors (PDX1, MAFA, BETA2, and ATF2) and the specific elements within the insulin promoter site [3,26,27]. In order to enhance the understanding of T2D pathophysiology, the regulatory effects of these transcription factors will need to be investigated in the future. The model can be further improved by considering the parameters related to transcription, mRNA stability and translation as a function of glucose to capture the dynamics of insulin synthesis in different glucose concentrations. Despite the limitations, the current model identifies crucial factors whose abnormalities could lead to either Type 2 diabetes (T2D) or hyperinsulinemic hypoglycemia.

In conclusion, the present study proposed a minimal model for insulin synthesis and secretion of insulin granules to understand the pathophysiology of T2D and hyperinsulinemic hypoglycemia. We observed that impairment in insulin synthesis (translation and transcription) could only be compensated on a smaller scale by many-fold changes in parameters representing insulin granule trafficking and exocytosis. Even many-fold changes in those parameters do not compensate for impairment in insulin synthesis (translation and transcription) on a larger scale (insulinoma). In contrast, impairment in insulin granule trafficking and exocytosis processes could be compensated by more reasonable changes in parameters representing insulin synthesis (translation and transcription) and hence needs further exploration.

Declaration of Competing Interest

The authors declare that they have no competing interests.

Data availability

No data was used for the research described in the article.

Acknowledgments

Research of AP is supported by University Grants Commission (11-04-2016-423482) Govt. of India. Research of JK is supported by the THSTI PhD Fellowship.

A. Description on parameter estimation from literature

Numerical value of δ_1*:* The half-life ($t_{1/2}$) of insulin mRNA depends on glucose concentration, and the value is 29 h and 77 h, respectively, at low and high glucose levels [15]. We calculated the degradation rate of insulin mRNA using the following equation

$$\delta_1 = \frac{ln(2)}{t_{1/2}} \tag{A.1}$$

The obtained values for δ_1 were 3.98×10^{-4} min^{-1} and 1.5×10^{-4} min^{-1}, respectively, at low and high glucose concentrations.

Numerical value of α_1*:* The mRNA expression value of insulin genes is 126,753 in tpm counts [30], so we used this value as the steady state value of M (M^*). We assumed that the system would always stay in a steady state at low glucose concentration, and the high glucose would act as a stimulus in the system. Thus, the value of α_1 at the low glucose setting was calculated from equation $M^* = \frac{\alpha_1}{\delta_1}$, and the obtained value was 50.4934 tpm min^{-1}.

It was reported that prolonged glucose stimulation (24 h) resulted in ~2-fold increase in insulin mRNA level (M) [14]. By solving the first equation of the system (9), we obtained

$$M(t) = \frac{\alpha_1}{\delta_1}(1 - e^{-\delta_1 t}) + M(0)e^{-\delta_1 t} \tag{A.2}$$

Now, we have information that $M(t_1) = 2 \times M(0)$ at $t = t_1$=24 h. Putting these values in Eq. (A.2), we get

$$2M(0) = \frac{\alpha_1}{\delta_1}(1 - e^{-\delta_1 t_1}) + M(0)e^{-\delta_1 t_1}$$

$$\Rightarrow M(0)(2 - e^{-\delta_1 t_1}) = \frac{\alpha_1}{\delta_1}(1 - e^{-\delta_1 t_1})$$

$$\Rightarrow \alpha_1 = \frac{M(0)\delta_1(2 - e^{-\delta_1 t_1})}{(1 - e^{-\delta_1 t_1})} \tag{A.3}$$

Finally, we put $M(0)$=126753, t_1=24 h and $\delta_1 = 1.5 \times 10^{-4}$ in Eq. (A.3) and obtained $\alpha_1 = 116.89$ for the high glucose model simulation.

B. Proof of the Result 1.

(i) By setting $X = (M, P, R, \gamma, D, D_{IR}, \rho)^T \in \mathbf{R}^7_+$ and $F(X) = [F_1(X), F_2(X), F_3(X), F_4(X), F_5(X), F_6(X), F_7(X)]^T$, Eq. (9) can be written as the system

$$\dot{X} = F(X), \tag{A.4}$$

together with initial conditions $X(0) = X_0 \in \mathbf{R}^7_+$. It is easy to check that whenever choosing $X(0) \in \mathbf{R}^7_+$ with $X_i = 0$, for $i = 1, \ldots, 7$, then $F_i(X)|_{X_i=0} \geq 0$. Due to the lemma of Nagumo [52], any solution of Eq. (A.4) with $X_0 \in \mathbf{R}^7_+$, say $X(t) = X(t; X_0)$, is such that $X(t) \in \mathbf{R}^7_+$ for all $t > 0$. Hence, the interior $\mathbf{R}^7_+$ is invariant for system (9).

(ii) From the first equation of (9), we get

$$\frac{dM}{dt} + \delta_1 M = \alpha_1$$

From the theory of differential inequalities [53], we then obtained

$$0 \leq M(t) \leq \frac{\alpha_1}{\delta_1}(1 - e^{-\delta_1 t}) + M(0)e^{-\delta_1 t}$$

From which we get,

$$M(t) \leq M_1, \forall t \geq 0 \tag{A.5}$$

where, $M_1 = \frac{\alpha_1}{\delta_1} + M(0)$.

From the second equation of (9), we get

$$\begin{aligned}\frac{dP}{dt} &= \nu M - \delta_2 P - kP\rho D_{IR}\\ &\le \nu M - \delta_2 P\\ &\le \nu M_1 - \delta_2 P\end{aligned}$$

Thus we obtain,

$$\frac{dP}{dt} + \delta_2 P \le \nu M_1$$

From the theory of differential inequalities [53], we get

$$0 \le P(t) \le \frac{\nu M_1}{\delta_2}(1 - e^{-\delta_2 t}) + P(0)e^{-\delta_2 t}$$

From which we get,

$$P(t) \le P_1, \forall t \ge 0 \tag{A.6}$$

where, $P_1 = \frac{\nu M_1}{\delta_2} + P(0)$.

From the fourth equation of (9), we get

$$\frac{d\gamma}{dt} + \eta\gamma = \eta(\gamma_b + \alpha_2)$$

By solving this we obtained

$$\gamma(t) = (\gamma_b + \alpha_2)(1 - e^{-\eta t}) + \gamma(0)e^{-\eta t}$$

From which we get,

$$l_1 \le \gamma(t) \le H_1, \forall t \ge 0 \tag{A.7}$$

where, $l_1 = \gamma_b + \alpha_2$ and $H_1 = \gamma_b + \alpha_2 + \gamma(0)$.

From the seventh equation of (9), we get

$$\begin{aligned}\frac{d\rho}{dt} + \zeta\rho &= \zeta\left(\rho_b + k_\rho(\gamma - \gamma_b)\right)\\ &\le \zeta\left(\rho_b + k_\rho(H_1 - \gamma_b)\right)\end{aligned}$$

From the theory of differential inequalities [53], we obtained

$$0 \le \rho(t) \le \left(\rho_b + k_\rho(H_1 - \gamma_b)\right)(1 - e^{-\zeta t}) + \rho(0)e^{-\zeta t}$$

From which we get,

$$\rho(t) \le H_2, \forall t \ge 0 \tag{A.8}$$

where, $H_2 = \left(\rho_b + k_\rho(H_1 - \gamma_b)\right) + \rho(0)$.

From the sixth equation of (9), we have

$$\frac{dD_{IR}}{dt} = k_1^+(C_T - D_{IR})D - k_1^- D_{IR} - \rho D_{IR} \tag{A.9}$$

Let us assume, for any instance $t_1 \ge 0$ the value $D_{IR}(t_1) = C_T$. Then from Eq. (A.9) we have

$$\frac{dD_{IR}}{dt}|_{t=t_1} = -(k_1^- + \rho)C_T < 0$$

Thus, the value of D_{IR} cannot crosses the threshold value C_T. Hence, $D_{IR}(t_1) < C_T$. Let us assume, $[D_{IR}]_{\max} = C_T - \epsilon$, where $\epsilon > 0$. From the third equation of (9), we get

$$\begin{aligned}\frac{dR}{dt} &= kP\rho D_{IR} - \gamma R\\ &\le kP\rho D_{IR} - l_1 R\end{aligned}$$

Thus,

$$\frac{dR}{dt} + l_1 R \le kP_1 C_T H_2$$

From the theory of differential inequalities [53], we obtained

$$0 \le R(t) \le \frac{kP_1 C_T H_2}{l_1}(1 - e^{-l_1 t}) + R(0)e^{-l_1 t}$$

From which we get,

$$R(t) \leq R_1, \forall t \geq 0 \tag{A.10}$$

where, $R_1 = \frac{kP_1C_TH_2}{l_1} + R(0)$.

From the fifth equation of (9), we get

$$\begin{aligned}\frac{dD}{dt} &= \gamma R - k_1^+(C_T - D_{IR})D + k_1^- D_{IR} \\ &\leq H_1R_1 - k_1^+\epsilon D + k_1^- C_T\end{aligned}$$

Thus we obtain,

$$\frac{dD}{dt} + k_1^+\epsilon D \leq H_1R_1 + k_1^- C_T$$

From the theory of differential inequalities [53], we obtained

$$0 \leq D(t) \leq \frac{H_1R_1 + k_1^- C_T}{k_1^+\epsilon}(1 - e^{-k_1^+\epsilon t}) + R(0)e^{-k_1^+\epsilon t}$$

Thus,

$$D(t) \leq D_1, \forall t \geq 0 \tag{A.11}$$

where, $D_1 = \frac{H_1R_1 + k_1^- C_T}{k_1^+\epsilon} + D(0)$.

Hence, this ensures the existence of a bounded region $\Gamma \in \mathbf{R}_+^7$ such that for any initial values $(M(0), P(0), R(0), \gamma(0), D(0), D_{IR}(0), \rho(0))^T$, solutions of the system (9) will always remain within the region Γ. This completes the proof.

C. Proof of the Result 2.

The equilibrium points of the system (9) was obtained by solving the following simultaneous algebraic equation

$$\begin{aligned}\alpha_1 - \delta_1 M^* &= 0, \\ \nu M^* - \delta_2 P^* - kP^*\rho D_{IR}^* &= 0, \\ kP^*\rho D_{IR}^* - \gamma^* R^* &= 0, \\ \eta(-\gamma^* + \gamma_b + \alpha_2) &= 0, \\ \gamma^* R^* - k_1^+\left(C_T - D_{IR}^*\right)D^* + k_1^- D_{IR}^* &= 0, \\ k_1^+\left(C_T - D_{IR}^*\right)D^* - k_1^- D_{IR}^* - \rho D_{IR}^* &= 0, \\ \zeta\left(-\rho^* + \rho_b + k_\rho(\gamma^* - \gamma_b)\right) &= 0.\end{aligned} \tag{A.12}$$

By solving the above simultaneous algebraic Eq. (A.12), we obtained

I. one non-interior equilibrium point, $E_{B0} \equiv (M_0^*, P_0^*, 0, \gamma_0^*, 0, 0, \rho_0^*)$, where $M_0^* = \frac{\alpha_1}{\delta_1}, P_0^* = \frac{\nu\alpha_1}{\delta_1\delta_2}, \gamma_0^* = \gamma_b + \alpha_2, \rho_0^* = \rho_b + k_\rho\alpha_2$ which exists for all parameter values, and

II. one interior equilibrium point, namely $E^* \equiv (M^*, P^*, R^*, \gamma^*, D^*, D_{IR}^*, \rho^*)$ is given by $M^* = \frac{\alpha_1}{\delta_1}$, $P^* = \frac{1}{k}$, $R^* = \frac{k\nu\alpha_1 - \delta_1\delta_2}{k\delta_1(\gamma_b + \alpha_2)}$, $\gamma^* = \gamma_b + \alpha_2$, $D^* = \frac{(k\nu\alpha_1 - \delta_1\delta_2)(\rho_b + k_\rho\alpha_2 + k_1^-)}{k_1^+[C_Tk\delta_1(\rho_b + k_\rho\alpha_2) - (k\nu\alpha_1 - \delta_1\delta_2)]}$, $D_{IR}^* = \frac{k\nu\alpha_1 - \delta_1\delta_2}{k\delta_1(\rho_b + k_\rho\alpha_2)}$ and $\rho^* = \rho_b + k_\rho\alpha_2$. E^* exists if (i) $(k\nu\alpha_1 - \delta_1\delta_2) > 0$ and (ii) $C_Tk\delta_1(\rho_b + k_\rho\alpha_2) > (k\nu\alpha_1 - \delta_1\delta_2)$.

To study the local stability properties of the equilibrium points we computed the Jacobian matrix (J) of system (9) around an arbitrary point $(M, P, R, \gamma, D, D_{IR}, \rho)$. It has the form

$$J = \begin{bmatrix} -\delta_1 & 0 & 0 & 0 & 0 & 0 & 0 \\ \nu & -(\delta_2 + k\rho D_{IR}) & 0 & 0 & 0 & -kP\rho & -kPD_{IR} \\ 0 & k\rho D_{IR} & -\gamma & -R & 0 & kP\rho & kPD_{IR} \\ 0 & 0 & 0 & -\eta & 0 & 0 & 0 \\ 0 & 0 & \gamma & R & -k_1^+(C_T - D_{IR}) & k_1^+D + k_1^- & 0 \\ 0 & 0 & 0 & 0 & k_1^+(C_T - D_{IR}) & -(k_1^+D + k_1^- + \rho) & -D_{IR} \\ 0 & 0 & 0 & \zeta k_\rho & 0 & 0 & -\zeta \end{bmatrix} \tag{A.13}$$

At the non-interior equilibrium point E_{B0}, the Jacobian becomes

$$J_{B_0} = \begin{bmatrix} -\delta_1 & 0 & 0 & 0 & 0 & 0 & 0 \\ \nu & -\delta_2 & 0 & 0 & 0 & -kP_0^*\rho_0^* & 0 \\ 0 & 0 & -\gamma_0^* & 0 & 0 & kP_0^*\rho_0^* & 0 \\ 0 & 0 & 0 & -\eta & 0 & 0 & 0 \\ 0 & 0 & \gamma_0^* & 0 & -k_1^+C_T & k_1^- & 0 \\ 0 & 0 & 0 & 0 & k_1^+C_T & -(k_1^- + \rho_0^*) & 0 \\ 0 & 0 & 0 & \zeta k_\rho & 0 & 0 & -\zeta \end{bmatrix}$$

The eigenvalues of J_{B_0} are λ_{0i}'s, $i = 1$ to 7, where $\lambda_{01} = -\delta_1 < 0$, $\lambda_{02} = -\delta_2 < 0$, $\lambda_{04} = -\eta < 0$, $\lambda_{07} = -\zeta < 0$ and λ_{03}, λ_{05}, λ_{06} are given by the roots of the equation

$$\lambda^3 + A_1\lambda^2 + A_2\lambda + A_3 = 0, \tag{A.14}$$

where,

$A_1 = (k_1^+C_T + k_1^- + \rho_0^* + \gamma_0^*) > 0$, $A_2 = k_1^+C_T\rho_0^* + \gamma_0^*(k_1^+C_T + k_1^- + \rho_0^*) > 0$ and $A_3 = k_1^+C_T\rho_0^*\gamma_0^*(1 - kP_0^*)$.

According to Routh-Hurwitz criterion, E_{B0} will be locally asymptotically stable if

(i) $A_n > 0$, $(n = 1, 2, 3)$,

(ii) $A_1A_2 - A_3 = (k_1^+C_T + k_1^- + \rho_0^*)\left(k_1^+C_T\rho_0^* + \gamma_0^*(k_1^+C_T + k_1^- + \rho_0^*) + \gamma_0^{*2}\right) + kk_1^+C_T\rho_0^*\gamma_0^*P_0^* > 0$.

Therefore E_{B0} will be locally asymptotically stable if $A_3 > 0$, i.e. $kv\alpha_1 < \delta_1\delta_2$.

At the interior equilibrium point E^*, the Jacobian becomes

$$J^* = \begin{bmatrix} -\delta_1 & 0 & 0 & 0 & 0 & 0 & 0 \\ v & -(\delta_2 + k\rho^*D_{IR}^*) & 0 & 0 & 0 & -kP^*\rho^* & -kP^*D_{IR}^* \\ 0 & k\rho^*D_{IR}^* & -\gamma^* & -R^* & 0 & kP^*\rho^* & kP^*D_{IR}^* \\ 0 & 0 & 0 & -\eta & 0 & 0 & 0 \\ 0 & 0 & \gamma^* & R^* & -k_1^+(C_T - D_{IR}^*) & k_1^+D^* + k_1^- & 0 \\ 0 & 0 & 0 & 0 & k_1^+(C_T - D_{IR}^*) & -(k_1^+D^* + k_1^- + \rho^*) & -D_{IR}^* \\ 0 & 0 & 0 & \zeta k_\rho & 0 & 0 & -\zeta \end{bmatrix}$$

The eigenvalues of J^* are λ_i's, $i = 1$ to 7, where $\lambda_1 = -\delta_1 < 0$, $\lambda_4 = -\eta < 0$, $\lambda_7 = -\zeta < 0$ and λ_2, λ_3, λ_5, λ_6 are given by the roots of the equation

$$\lambda^4 + A_1\lambda^3 + A_2\lambda^2 + A_3\lambda + A_4 = 0 \tag{A.15}$$

where,

$$\begin{aligned} A_1 &= (B + C + \gamma^*) > 0, \\ A_2 &= (A\rho^* + (B + C)\gamma^* + BC) > 0, \\ A_3 &= (A\gamma^*\rho^* - kAP^*\gamma^*\rho^* + AB\rho^* + BC\gamma^*), \\ A_4 &= (AB\gamma^*\rho^* - \delta_2 kAP^*\gamma^*\rho^*). \end{aligned}$$

The values of A, B and C are given by

$A = k_1^+(C_T - D_{IR}^*) > 0$

$B = (\delta_2 + k\rho^*D_{IR}^*) > 0$

$C = k_1^+(C_T - D_{IR}^*) + (k_1^+D^* + k_1^- + \rho^*) = (A + k_1^+D + k_1^- + \rho^*) > 0$

Thus, according to Routh-Hurwitz criterion, E^* will be locally asymptotically stable if

$$\begin{aligned} &a.\ A\gamma^*\rho^* + AB\rho^* + BC\gamma^* > kAP^*\gamma^*\rho^*, \\ &b.\ B > \delta_2 kP^*, \\ &c.\ (B + C + \gamma^*)(A\rho^* + (B + C)\gamma^* + BC) > (A\gamma^*\rho^* - kAP^*\gamma^*\rho^* + AB\rho^* + BC\gamma^*), \\ &d.\ (B + C + \gamma^*)(A\rho^* + (B + C)\gamma^* + BC)(A\gamma^*\rho^* - kAP^*\gamma^*\rho^* + AB\rho^* + BC\gamma^*) > \\ &\quad (A\gamma^*\rho^* - kAP^*\gamma^*\rho^* + AB\rho^* + BC\gamma^*)^2 + (B + C + \gamma^*)^2(AB\gamma^*\rho^* - \delta_2 kAP^*\gamma^*\rho^*). \end{aligned}$$

If all of these conditions are satisfied then E^* will be globally asymptotically stable, since according to the existence criterion of E^*, E_{B0} will be unstable.

References

[1] P. Sonksen, J. Sonksen, Insulin: understanding its action in health and disease, Br. J. Anaesth. 85 (1) (2000) 69–79.

[2] G. Wilcox, Insulin and insulin resistance, Clin. Biochem. Rev. 26 (2) (2005) 19.

[3] Z. Fu, E. R Gilbert, D. Liu, Regulation of insulin synthesis and secretion and pancreatic beta-cell dysfunction in diabetes, Curr. Diabetes Rev. 9 (1) (2013) 25–53.

[4] J.J. Meier, R.C. Bonadonna, Role of reduced β-cell mass versus impaired β-cell function in the pathogenesis of type 2 diabetes, Diabetes Care 36 (Supplement_2) (2013) S113–S119.

[5] Y. Yang, Z. Cai, Z. Pan, F. Liu, D. Li, Y. Ji, J. Zhong, H. Luo, S. Hu, L. Song, et al., Rheb1 promotes glucose-stimulated insulin secretion in human and mouse β-cells by upregulating glut expression, Metabolism 123 (2021) 154863.

[6] J.-M. Guettier, P. Gorden, Insulin secretion and insulin-producing tumors, Expert Rev. Endocrinol. Metab. 5 (2) (2010) 217–227.

[7] J.-M. Guettier, P. Gorden, Hypoglycemia, Endocrinology and Metab. Clin. 35 (4) (2006) 753–766.

[8] D.L. Curry, L.L. Bennett, G.M. Grodsky, Dynamics of insulin secretion by the perfused rat pancreas, Endocrinology 83 (3) (1968) 572–584.

[9] J.-C. Henquin, N. Ishiyama, M. Nenquin, M.A. Ravier, J.-C. Jonas, Signals and pools underlying biphasic insulin secretion, Diabetes 51 (suppl_1) (2002) S60–S67.

[10] Z. Wang, D.C. Thurmond, Mechanisms of biphasic insulin-granule exocytosis–roles of the cytoskeleton, small GTPases and snare proteins, J. Cell. Sci. 122 (7) (2009) 893–903.

[11] J.-C. Henquin, Triggering and amplifying pathways of regulation of insulin secretion by glucose, Diabetes 49 (11) (2000) 1751–1760.

[12] S. Daniel, M. Noda, S.G. Straub, G. Sharp, Identification of the docked granule pool responsible for the first phase of glucose-stimulated insulin secretion, Diabetes 48 (9) (1999) 1686–1690.

[13] M. Omar-Hmeadi, O. Idevall-Hagren, Insulin granule biogenesis and exocytosis, Cell. Mol. Life Sci. 78 (5) (2021) 1957–1970.

[14] B. Wicksteed, C. Alarcon, I. Briaud, M.K. Lingohr, C.J. Rhodes, Glucose-induced translational control of proinsulin biosynthesis is proportional to pre-proinsulin mRNA levels in islet β-cells but not regulated via a positive feedback of secreted insulin, J. Biol. Chem. 278 (43) (2003) 42080–42090.
[15] M. Welsh, D.A. Nielsen, A.J. MacKrell, D.F. Steiner, Control of insulin gene expression in pancreatic beta-cells and in an insulin-producing cell line, RIN-5F cells. ii. regulation of insulin mRNA stability, J. Biol. Chem. 260 (25) (1985) 13590–13594.
[16] K.E. Rohli, C.K. Boyer, S.E. Blom, S.B. Stephens, Nutrient regulation of pancreatic islet β-cell secretory capacity and insulin production, Biomolecules 12 (2) (2022) 335.
[17] A. Paul, P.N. Das, S. Chatterjee, A minimal model of glucose-stimulated insulin secretion process explores factors responsible for the development of type 2 diabetes, Appl. Math. Model. 108 (2022) 408–426.
[18] A. Mari, A. Tura, E. Grespan, R. Bizzotto, Mathematical modeling for the physiological and clinical investigation of glucose homeostasis and diabetes, Front. Physiol. 11 (2020) 1548.
[19] R.V. Overgaard, K. Jelic, M. Karlsson, J.E. Henriksen, H. Madsen, Mathematical beta cell model for insulin secretion following IVGTT and OGTT, Ann. Biomed. Eng. 34 (8) (2006) 1343–1354.
[20] A. Bertuzzi, S. Salinari, G. Mingrone, Insulin granule trafficking in β-cells: mathematical model of glucose-induced insulin secretion, Am. J. Physiol.-Endocrinol.Metab. 293 (1) (2007) E396–E409.
[21] E. Grespan, T. Giorgino, S. Arslanian, A. Natali, E. Ferrannini, A. Mari, Defective amplifying pathway of β-cell secretory response to glucose in type 2 diabetes: integrated modeling of in vitro and in vivo evidence, Diabetes 67 (3) (2018) 496–506.
[22] N. Kaiser, G. Leibowitz, R. Nesher, Glucotoxicity and β-cell failure in type 2 diabetes mellitus, J. Pediatr. Endocrinol. Metab. 16 (1) (2003) 5–22.
[23] S. Barg, L. Eliasson, E. Renstrom, P. Rorsman, A subset of 50 secretory granules in close contact with L-type Ca2+ channels accounts for first-phase insulin secretion in mouse β-cells, Diabetes 51 (suppl_1) (2002) S74–S82.
[24] P. Rorsman, E. Renström, Insulin granule dynamics in pancreatic beta cells, Diabetologia 46 (8) (2003) 1029–1045.
[25] T. Bock, K. Svenstrup, B. Pakkenberg, K. Buschard, Unbiased estimation of total β-cell number and mean β-cell volume in rodent pancreas, APMIS 107 (7–12) (1999) 791–799.
[26] D. Melloul, S. Marshak, E. Cerasi, Regulation of insulin gene transcription, Diabetologia 45 (3) (2002) 309–326.
[27] S.-i. Han, K. Yasuda, K. Kataoka, ATF2 interacts with β-cell-enriched transcription factors, MafA, Pdx1, and Beta2, and activates insulin gene transcription, J. Biol. Chem. 286 (12) (2011) 10449–10456.
[28] V. Poitout, D. Hagman, R. Stein, I. Artner, R.P. Robertson, J.S. Harmon, Regulation of the insulin gene by glucose and fatty acids, J. Nutr. 136 (4) (2006) 873–876.
[29] M. Weiss, D.F. Steiner, L.H. Philipson, Insulin biosynthesis, secretion, structure, and structure-activity relationships (2015).
[30] B. Kutlu, D. Burdick, D. Baxter, J. Rasschaert, D. Flamez, D.L. Eizirik, N. Welsh, N. Goodman, L. Hood, Detailed transcriptome atlas of the pancreatic beta cell, BMC Med. Genomics 2 (1) (2009) 1–11.
[31] G.M. Grodsky, et al., A threshold distribution hypothesis for packet storage of insulin and its mathematical modeling, J. Clin. Invest. 51 (8) (1972) 2047–2059.
[32] P.A. Halban, K.S. Polonsky, D.W. Bowden, M.A. Hawkins, C. Ling, K.J. Mather, A.C. Powers, C.J. Rhodes, L. Sussel, G.C. Weir, β-cell failure in type 2 diabetes: postulated mechanisms and prospects for prevention and treatment, J. Clin. Endocrinol.Metab. 99 (6) (2014) 1983–1992.
[33] A. Paul, S. Azhar, P.N. Das, N. Bairagi, S. Chatterjee, Elucidating the metabolic characteristics of pancreatic β-cells from patients with type 2 diabetes (T2D) using a genome-scale metabolic modeling, Comput. Biol. Med. 144 (2022) 105365.
[34] J.-C. Henquin, Glucose-induced insulin secretion in isolated human islets: does it truly reflect β-cell function in vivo? Mol. Metab. 48 (2021) 101212.
[35] S.M. Blower, H. Dowlatabadi, Sensitivity and uncertainty analysis of complex models of disease transmission: an HIV model, as an example, Int. Stat. Rev./Revue Internationale de Statistique (1994) 229–243.
[36] S. Marino, D.E. Kirschner, A multi-compartment hybrid computational model predicts key roles for dendritic cells in tuberculosis infection, Computation 4 (4) (2016) 39.
[37] S. Marino, I.B. Hogue, C.J. Ray, D.E. Kirschner, A methodology for performing global uncertainty and sensitivity analysis in systems biology, J. Theor. Biol. 254 (1) (2008) 178–196.
[38] D. Prídavková, M. Samoš, R. Kyčina, K. Adamicová, M. Kalman, M. Belicová, M. Mokáň, Insulinoma presenting with postprandial hypoglycemia and a low body mass index: a case report, World J. Clin. Cases 8 (18) (2020) 4169.
[39] G.C. Weir, S. Bonner-Weir, Five stages of evolving beta-cell dysfunction during progression to diabetes, Diabetes 53 (suppl 3) (2004) S16–S21.
[40] A.V. Matveyenko, P. Butler, Relationship between β-cell mass and diabetes onset, Diabetes Obesity Metab. 10 (2008) 23–31.
[41] H. Sasaki, Y. Saisho, J. Inaishi, Y. Watanabe, T. Tsuchiya, M. Makio, M. Sato, M. Nishikawa, M. Kitago, T. Yamada, et al., Reduced beta cell number rather than size is a major contributor to beta cell loss in type 2 diabetes, Diabetologia (2021) 1–6.
[42] P. Iglesias, J.J. Díez, Management of endocrine disease: a clinical update on tumor-induced hypoglycemia, Eur. J. Endocrinol. 170 (4) (2014) R147–R157.
[43] C.M. Cohrs, J.K. Panzer, D.M. Drotar, S.J. Enos, N. Kipke, C. Chen, R. Bozsak, E. Schöniger, F. Ehehalt, M. Distler, et al., Dysfunction of persisting β cells is a key feature of early type 2 diabetes pathogenesis, Cell Rep. 31 (1) (2020) 107469.
[44] J.C. Koster, M.A. Permutt, C.G. Nichols, Diabetes and insulin secretion: the ATP-sensitive K+ channel (KATP) connection, Diabetes 54 (11) (2005) 3065–3072.
[45] Y.I. Kitamura, T. Kitamura, J.-P. Kruse, J.C. Raum, R. Stein, W. Gu, D. Accili, FoxO1 protects against pancreatic β cell failure through NeuroD and MafA induction, Cell Metab. 2 (3) (2005) 153–163.
[46] M.F. Brereton, M. Iberl, K. Shimomura, Q. Zhang, A.E. Adriaenssens, P. Proks, I.I. Spiliotis, W. Dace, K.K. Mattis, R. Ramracheya, et al., Reversible changes in pancreatic islet structure and function produced by elevated blood glucose, Nat. Commun. 5 (1) (2014) 1–11.
[47] H.S. Spijker, H. Song, J.H. Ellenbroek, M.M. Roefs, M.A. Engelse, E. Bos, A.J. Koster, T.J. Rabelink, B.C. Hansen, A. Clark, et al., Loss of β-cell identity occurs in type 2 diabetes and is associated with islet amyloid deposits, Diabetes 64 (8) (2015) 2928–2938.
[48] C. Talchai, S. Xuan, H.V. Lin, L. Sussel, D. Accili, Pancreatic β cell dedifferentiation as a mechanism of diabetic β cell failure, Cell 150 (6) (2012) 1223–1234.
[49] G.C. Weir, C. Aguayo-Mazzucato, S. Bonner-Weir, β-cell dedifferentiation in diabetes is important, but what is it? Islets 5 (5) (2013) 233–237.
[50] M.E. Doyle, J.M. Egan, Mechanisms of action of glucagon-like peptide 1 in the pancreas, Pharmacol. Ther. 113 (3) (2007) 546–593.
[51] D. Hinnen, Glucagon-like peptide 1 receptor agonists for type 2 diabetes, Diabetes Spectr. 30 (3) (2017) 202–210.
[52] M. Nagumo, Über die lage der integralkurven gewöhnlicher differentialgleichungen, in: Proceedings of the Physico, in: 3rd Series, Vol. 24, Mathematical Society of Japan, 1942, pp. 551–559.
[53] G. Birkhoff, G.-C. Rota, Ordinary Differential Equations, John Wiley & Sons, 1978.